

LEVEL
12

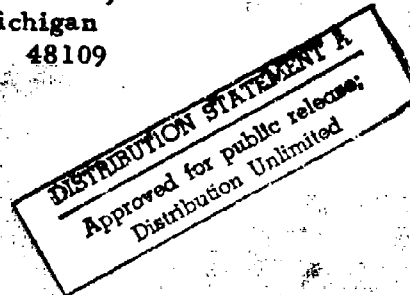
Report No. 018209-3-F

INVESTIGATION OF AERODYNAMIC STALL ALLEVIATION
ON A SWEEP PLANFORM WING USING LEADING EDGE MODIFICATIONS

Roger W. Van Gunst
Shreekant Agrawal
Brian Meyer

DTIC
SELECTED
JUL 11 1981
S C D

Aircraft Research Laboratory
The University of Michigan
Ann Arbor, Michigan 48109



Prepared under Contract No. N000167-80-C-0058

for

David Taylor Naval Ship Research and Development Center
Bethesda, Maryland 20084

and

Naval Air Systems Command
Washington, D. C. 20361

May 1981

81 7 10 057

ONE FILE COPY

12

INVESTIGATION OF AERODYNAMIC STALL ALLEVIATION
ON A SWEPT PLANFORM WING USING LEADING EDGE MODIFICATIONS

Roger W. Van Gunst
Shreekant Agrawal
Brian Meyer

Aircraft Research Laboratory
The University of Michigan
Ann Arbor, Michigan 48109

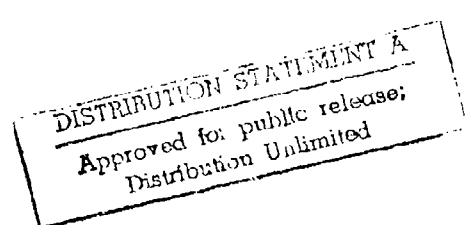


Prepared under Contract No. N000167-80-C-0058
for
David Taylor Naval Ship Research and Development Center
Bethesda, Maryland 20084

and

Naval Air Systems Command
Washington, D. C. 20361

May 1981



REPORT DOCUMENTATION PAGE		READ INSTRUCTIONS BEFORE COMPLETING FORM
1. REPORT NUMBER 018209-3-F	2. GOVT ACCESSION NO. AD-A101239	3. RECIPIENT'S CATALOG NUMBER
4. TITLE (If different from Report) INVESTIGATION OF AERODYNAMIC STALL ALLEVIATION ON A SWEPT PLANFORM WING USING LEADING EDGE MODIFICATIONS.		5. TYPE OF REPORT & PERIOD COVERED Final Report 10 April 1980 - 5 January 1981
6. AUTHOR(s) Roger W. Van Gunst Shreekant Agrawal Brian Meyer	7. CONTRACT OR GRANT NUMBER(s) N000167-80-C-0058	8. PERFORMING ORG. REPORT NUMBER
9. PERFORMING ORGANIZATION NAME AND ADDRESS Aircraft Research Laboratory The University of Michigan Ann Arbor, Michigan 48109	10. PROGRAM ELEMENT, PROJECT, TASK AREA & WORK UNIT NUMBERS 10168	11. REPORT DATE May 1981
12. MONITORING AGENCY NAME & ADDRESS (if different from Controlling Office) David Taylor Naval Ship Research and Development Center Bethesda, Maryland 20084	13. SECURITY CLASS. (of this report) Unclassified	14. DECLASSIFICATION/DOWNGRADING SCHEDULE
15. DISTRIBUTION STATEMENT (of this Report) Approved for public release; distribution unlimited	16. DISTRIBUTION STATEMENT (of the abstract entered in Block 20, if different from Report)	
17. SUPPLEMENTARY NOTES		
18. KEY WORDS (Continue on reverse side if necessary and identify by block number) vortex generation stall alleviation leading edge modification		
19. ABSTRACT (Continue on reverse side if necessary and identify by block number) A wind tunnel investigation was conducted to determine the effect of leading edge modifications on the stall characteristics of a swept planform wing. The modifications consisted of openings in the leading edge which generated a vortex pattern over the wing surface. The force/moment results showed that a 33 percent increase in stall angle of attack could be achieved with the leading edge modifications. A maximum lift coefficient comparable to that of the baseline wing was also		

Unclassified

SECURITY CLASSIFICATION OF THIS PAGE(When Data Entered)

Block 20 Continued

achieved with the modifications. Evidence of interference between the modification-generated flow field and the wind tunnel upper surface indicated that these high angle of attack results are a conservative evaluation of the modification's lift enhancement potential. The nose up pitching moment at stall was moderated by the leading edge modifications and no increase in drag occurred below 19 degrees angle of attack.

Preliminary flow visualization results indicate that these force/moment characteristics associated with the leading edge modifications are caused by vortices formed on each side of the modification opening.

The test results indicate that the leading edge modifications have the potential for increasing the maneuvering capability and stall margin of airplane flight operations.

Unclassified

SECURITY CLASSIFICATION OF THIS PAGE(When Data Entered)

SUMMARY

A wind tunnel investigation was conducted to determine the effect of leading edge modifications on the stall characteristics of a swept planform wing. The modifications consisted of openings in the leading edge which generated a vortex pattern over the wing surface.

The force/moment results showed that a 33 percent increase in stall angle of attack could be achieved with the leading edge modifications. A maximum lift coefficient comparable to that of the baseline wing was also achieved with the modifications. Evidence of interference between the modification-generated flow field and the wind tunnel upper surface indicated that these high angle of attack results are a conservative evaluation of the modification's lift enhancement potential. The nose up pitching moment at stall was moderated by the leading edge modifications and no increase in drag occurred below 19 degrees angle of attack.

Preliminary flow visualization results indicate that these force/moment characteristics associated with the leading edge modifications are caused by vortices formed on each side of the modification opening.

The test results indicate that the leading edge modifications have the potential for increasing the maneuvering capability and stall margin of airplane flight operations.

Accession No.	_____
NTIS Ref. #	_____
DTIC TAB	<input type="checkbox"/>
Unannounced	<input type="checkbox"/>
Justification _____	
By _____	
Distribution/ _____	
Availability Codes _____	
Avail and/or _____	
Dist	Special
A	

FOREWORD

The work described in this report was performed by the Aircraft Research Laboratory of The University of Michigan for the Naval Air Systems Command, Washington, D. C. and David Taylor Naval Ship Research and Development Center, Bethesda, MD under Contract Number N000167-80-C-0058. The research program was undertaken under the technical cognizance of Mr. D. G. Kirkpatrick (NAVAIR-320D) and Dr. T. C. Tai (DTNSRDC-1606).

TABLE OF CONTENTS

SUMMARY	ii
FOREWARD	iii
TABLE OF CONTENTS	iv
LIST OF FIGURES.	v
LIST OF SYMBOLS	vii
1. INTRODUCTION	1
2. DESCRIPTION OF WIND TUNNEL MODEL AND DATA ACQUISITION	2
2.1 Models	2
2.1.1 Straight Planform Wing	3
2.1.2 Swept Planform Wing	4
2.2 Data Acquisition.	5
3. WIND TUNNEL TESTS	7
3.1 Straight Planform Wing.	7
3.2 Swept Planform Wing	8
3.2.1 Preliminary Study	8
3.2.2 Lift Optimization Study	10
3.2.3 Reynolds Number Study	13
3.3 Flow Visualization Study	14
4. DISCUSSION OF RESULTS	16
CONCLUSIONS AND RECOMMENDATIONS	19
REFERENCES	21
APPENDIX A	54
APPENDIX B	56

LIST OF FIGURES

1.	Airfoil Section of Straight and Swept Wing Wind Tunnel Models	22
2.	Straight Planform Wing Model Mounted on the Wind Tunnel Balance Tripod Support	23
3.	Nomenclature for Geometry Features of Leading Edge Modification Inserts	24
4.	Leading Edge Inserts Used in the Straight Planform Wing Study with their Respective Modification Openings	25
5.	A Sketch of the 30 Degree Swept Wing with the Leading Edge Insert Station Designations	26
6.	Leading Edge Inserts Used in the Swept Planform Wing Study with their Respective Modification Openings	27
7.	Lift Characteristics Associated with Varying Insert Cut-Out Chord Dimension	31
8.	Lift Characteristics Associated with Three Teardrop Shape Modification Openings	32
9.	Lift Characteristics Associated with Teardrop and Elliptical Shape Insert Openings Compared with the Baseline Wing	33
10.	Comparison of Drag Characteristics Between Teardrop and Elliptical Shape Insert Openings	34
11.	Preliminary C_L vs α Optimization Results Using One Modification Opening	35
12.	Preliminary C_L vs α Optimization Results Using Two Insert Openings	36
13.	Swept Wing Leading Edge Inserts with Modified Opening Geometry Developed in the Lift Optimization Study	37
14.	Lift Optimization Results Achieved by Changing the Inboard Insert Opening Geometry	40
15.	Lift Characteristics Achieved with Various Modification Insert Configurations During the Optimization of the Swept Planform Wing	41

16.	Change in Drag Associated with the Leading Edge Modification Configuration of Test Run #275	42
17.	Comparison of the Pitching Moment Associated with the Leading Edge Modification Configuration of Test Run #275 with that of the Baseline Wing	43
18.	Comparison of Lift Characteristics Between the Modified and Baseline Wing and Upper and Lower Lift Readings in the α -Range of Wind Tunnel Wall Interference	44
19.	Comparison of Reynolds Number Effects Associated with the Modified and Baseline Swept Planform Wing	45
20.	Sketch of the Representative Flow Field Associated with a Leading Edge Modification Opening Located at the Wing Mid-Semispan Position	46
21.	Fluorescent Dye/ Oil Smear Contours Associated with One Leading Edge Insert Opening	47
22.	Fluorescent Dye/ Oil Smear Contours Associated with Two Leading Edge Insert Openings	51

LIST OF SYMBOLS

b	Half span length of wing
c	Wing chord
C_D	Drag coefficient of the wing
C_L	Lift coefficient of the wing
$C_{L_{max}}$	Maximum lift coefficient of the wing
C_M	Pitching moment coefficient about the wing MAC (Positive sense - nose up)
Re	Reynolds number
S	Surface area of the wing
α	Angle of attack of the wing (degrees)
α_{stall}	Angle of attack at which aerodynamic stall occurs
Λ	Sweep angle of wing
λ	Taper ratio of wing

ABBREVIATIONS

vs	Versus
cm	Centimeter/s
m	Meter/s
#	Number

1. INTRODUCTION

An exploratory research program was conducted by the Department of Aerospace Engineering at The University of Michigan in which wing leading edge modifications were studied for stall alleviation properties. These modifications were openings in the leading edge of the wing. The openings tested in the exploratory program were an outgrowth of the rectangular shaped openings used by Dr. R. Kroeger in his stall modification research (references 1, 2). The opening geometry of the modification used in this exploratory program differed from those used previously in that wing stubs and smooth surface contouring were added to the original opening. These modification features will be discussed in later sections of the report.

The force/moment data obtained in the exploratory study showed that an improved lift capability could be obtained with the new leading edge opening configurations. Relative to the unmodified wing, the leading edge opening modification results showed an increase of 20 percent in $C_{L_{max}}$ with a 95 percent increase in stall angle of attack. No significant change in pitching moment was observed and below 12 degrees angle of attack the modified wing showed no increase in drag.

Some preliminary work was also done in the exploratory study to identify a relationship between lift characteristics and the modification opening geometry. This study showed that predictable changes could be made to the lift vs α curve with changes in the modification opening geometry. This lift curve tailoring was used to maintain a positive lift

curve slope from 0 to 40 degrees with the straight planform wing wind tunnel model used in the exploratory study.

These results provided the motivation to explore the applicability of the leading edge modification openings to the swept planform wing.

The swept wing program was designed to study the high angle of attack lift enhancement capability of the leading edge modifications when incorporated on a 30 degree swept planform wing. Drag and pitching moment data was recorded to evaluate the changes caused by the modifications to these parameters. The first three weeks of the research program were used to continue two studies begun in the initial exploratory study. These studies dealt with the lift characteristics associated with changes made in the size and shape of the straight wing leading edge opening geometry.

2. DESCRIPTION OF WIND TUNNEL MODEL AND DATA ACQUISITION SYSTEM

2.1 Models

2.1.1 Straight Planform Wing

This model was the same as that used in the exploratory research study. It was a semispan wing attached to a circular endplate .91 m in diameter. The planform of this wing had the following characteristics:

1. $S = .63 \text{ m}^2$
2. $C = .47 \text{ m}$
3. $b = 1.32 \text{ m}$
4. $\lambda = 1$
5. $\Lambda = 0$
6. Washout = 2 degrees

The airfoil section consisted of a leading edge cuff attached to a 65₂-415 airfoil. A sketch of this section is shown in figure 1.

The model was constructed with an aluminum spar and frame. Foam material was used as a core with a fiberglass cover to provide a smooth, durable exterior surface. This model was mounted on the vertical post of the wind tunnel balance system by a tripod attachment as shown in figure 2. The angle of attack was adjusted by means of a motor driven worm gear system which raised or lowered the front attachment strut of the tripod mount.

A rectangular opening 13.33 cm wide by 8.89 cm deep was cut into the leading edge of the wing model. The inboard edge of this gap coincided with the mid-semispan location. Another rectangular gap 6.81 cm wide and 8.89 cm deep was cut into the wing root leading edge. Insert blocks,

having an identical cross section as the rectangular block which was removed, were mounted into the leading edge gap of the wing. Mylar tape and spackling compound were used to attain a smooth attachment between the insert and wing surface.

The desired modification opening was cut into the insert blocks. Thus each insert block had a unique leading edge modification opening configuration. The test results discussed in this report will be identified with the inserts used, in the wing model, for each test configuration. The features of these insert openings will be discussed in the report with the nomenclature given in the generalized planform view of figure 3. A summary of the leading edge configurations discussed in this report are given in Appendix A and B.

Figure 4 shows the leading edge inserts used in the straight planform wing study.

2.1.2 Swept Planform Wing

The model for this investigation was a semispan wing attached to a circular endplate with a .91 m diameter. The planform of this wing had the following characteristics:

1. $S = .62 \text{ m}^2$
2. $C = .55 \text{ m}$
3. $b = 1.14 \text{ m}$
4. $\lambda = 1$
5. $\Lambda = 30 \text{ degrees}$
6. Washout = 0 degrees

The wing model airfoil section was identical to that of the straight wing model described previously and shown in figure 1.

The model was constructed of wood. Plywood was used for the core and mahogany for the exterior material. Numerous applications of sanding sealer and paint provided a smooth exterior surface. The wing was mounted on the wind tunnel balance in the same manner as the straight wing model.

The leading edge of the swept wing model was divided into ten equal segments. Each segment was numbered consecutively from the wing root outboard. This arrangement is shown on the planform sketch of the swept wing model in figure 5. These leading edge segments were cut as necessary to accommodate the insert and location stipulated in the test plan. Other details of the insert blocks and their associated modification opening configurations have been discussed previously in the straight wing model section. Figure 6 shows the leading edge inserts used in the swept wing research program.

2.2 Data Acquisition

The wind tunnel used to conduct the tests of this study was a 1.52 by 2.13 meter, closed return tunnel having a contraction ratio of 15. Test speeds up to 76 meters/second can be achieved.

The tunnel is equipped with a six-component, external balance system located below the floor. Models are mounted on a vertical post that extends through an opening in the test section floor to a parallelogram linkage system which applies the model force/moment components to separate strain gage beams. The imbalance in voltage at each strain gage bridge is read by a millivolt meter and displayed in digital form on the master console. The strain gage output can also be recorded on paper tape and processed through

the data reduction program of a NOVA 840 minicomputer. This program incorporates standard wind tunnel corrections, as described in references 3 and 4 and reduces each data point to coefficient form.

The force/moment coefficient versus angle of attack plots obtained in this study were generated by data recordings taken in 2 degree intervals up to 20 degrees and then up to 44 degrees in 1 degree intervals. The plots shown in this report are duplications of the computer plots with identification symbols added at significant points on the respective curves.

3. WIND TUNNEL TESTS

3.1 Straight Planform Wing

The straight planform wing model was used to continue the investigation, of two modification opening parameters, in the exploratory study. These two parameters were the chordwise opening size and the shape of the modification opening.

In the exploratory study an initial opening of 1.11 cm was tested. A subsequent test series was conducted with opening sizes of 1.91 cm, 2.54 cm, 3.18 cm and 3.81 cm. The insensitivity of α_{stall} and $C_{L_{max}}$ shown in the results with increasing opening size indicated that chordwise openings of less than 1.11 cm were possible without significantly degrading these lift parameters. Thus a test series was conducted in this study with an initial chordwise opening size of .16 cm. Subsequent chordwise openings were tested at .32 cm, .48 cm, .64 cm, and .79 cm. The modification insert was designed so that each successive opening was cut on a lathe without changing any other geometry of the modification opening. A photograph of this insert is shown in figure 4(d). The wing stubs have been removed to show the back face surface and sides of the modification opening. The wing stubs were attached to the lateral sides of the opening for each data test run.

The test results of the four modification openings are shown in figure 7. Due to time limitations the openings of .95 cm and 1.11 cm were not completed in this test series and thus no conclusion can be drawn concerning optimum chordwise opening size. The data of figure 7

do show that lift is moderately sensitive to change in the chordwise opening but no trend can be identified which indicates a preferred opening size.

An elliptical shape modification opening was tested in the exploratory leading edge modification study. To obtain information on the sensitivity of lift to the modification opening shape, a teardrop shape opening was tested in the straight wing model. Three sizes of teardrop shape modification openings were tested. The inserts and their associated openings are shown in figure 4. The C_L vs α results obtained with each of the modification openings is shown in figure 8.

The C_L vs α results obtained with insert #12 were chosen as the best lift characteristics obtained in this test series. This lift result is compared with that of the baseline wing and the best lift result obtained with an elliptical shape modification opening (insert #10) in figure 9. The teardrop shape opening results show an increase in $C_{L_{max}}$ and α_{stall} relative to the baseline wing but reduced $C_{L_{max}}$ relative to the elliptical shape modification opening. The significant feature of this test series was the low drag exhibited by insert #12. Figure 10 compares the change in drag, relative to the baseline wing, of inserts #12 and #10. In the angle of attack range from 0 to 21 degrees the teardrop shape opening has a lower drag than the elliptical modification opening.

3.2 Swept Planform Wing

3.2.1 Preliminary Study

The swept wing leading edge modification opening tests began with one insert located at the wing root. Subsequent tests were

conducted with the insert located at successive outboard positions. The best lift curve results of this test series were obtained with run #241, #242 and #238. These results were obtained with insert #26 located at stations 5B/6A, 6A/6B and 6B/7B, respectively. Figure 11 shows a comparison of these test results. The results of run #242 were selected as representing the preliminary optimum lift characteristics obtainable with one leading edge modification opening.

An elliptical shape modification opening was used in these initial tests to maximize CL_{max} . The orientation of the modification opening back face surface relative to the wind tunnel longitudinal axis was studied to determine the sensitivity of lift to this modification parameter. This surface was parallel to the leading edge in insert #26. Insert #25 was fabricated with the back surface face perpendicular to the tunnel longitudinal axis. The other modification configuration features of insert #25 were patterned after those of insert #26. Both inserts were tested at the 6B/7A spanwise location. The force/moment results of these two insert configurations showed no significant differences. The insert opening back face configuration of insert #26 was used for the remainder of the swept wing study.

A test series was then conducted with insert #26 at the 6A/6B spanwise location and insert #30 mounted first at the wing root and then moved toward insert #26 with each subsequent test. The best results of this test series were obtained with test runs #248, #249 and #250. These test runs correlated with insert #30 being installed at the spanwise location of 2B/3A, 3A/3B and 3B/4A, respectively. The lift characteristics obtained with

these three configurations are shown in figure 12. The result of test run #249 was selected as representing the preliminary optimum lift modification obtainable with two leading edge modifications. Although the test configuration of run #248 attained a higher stall angle of attack, relative to run #249, the more pronounced negative lift curve slope located at the angle of attack of 23 and 32 degrees were evaluated as more than offsetting the increase in α_{stall} of test run #248.

3.2.2 Lift Optimization Study

The modification opening geometry of inserts #30 and #26 had not been tailored for lift performance in the swept wing model. The test program to this point had identified a preliminary optimum modification location for the two-insert configuration. It was now decided to iteratively change the modification opening geometry of these two inserts to achieve an increase in $C_{L_{max}}$ and α_{stall} . This optimization process was carried out in two stages. First the modification opening of the inboard insert (#30) was changed and that of the outboard insert (#26) was unaltered. Upon achieving a preliminary optimum opening geometry for the inboard insert, this was kept constant and the modification opening of the outboard insert (#26) was iteratively changed.

The primary modification opening features which were changed during these iterative optimization studies were the wing stub thickness, wing stub gap opening, and chordwise and spanwise opening located just aft the wing stubs. The filling and enlargement associated with these feature changes was accomplished with modelling clay whenever possible.

In this optimization study the lift values for each test angle of attack were hand recorded. Complete data reduction and plotting were only used for test runs where documentation was thought necessary for future analysis. No permanent documentation was made of the many iteration results obtained in the optimization process.

Following each test run, the data was analyzed and compared with the previous test results. From these comparisons successive iterations were identified, modelled and tested. This iterative process evolved the modified configuration opening of insert #30 shown in figure 13. A comparison of the lift characteristics obtained with this modified opening geometry of insert #30 and the unaltered opening of insert #26 is shown as test run #266 in figure 14. The wing configuration of test run #249 was identical to that of test run #266 with the exception that the insert #30 opening was not filled.

The second stage of this optimization study was then conducted with the preliminary optimum opening shape of the inboard insert held constant and iterative changes made to the opening of the outboard insert. During this test series the data indicated that a larger opening should be used in the outboard insert. Thus insert #31 was fabricated and used for the remainder of the test series. Successive changes to this insert evolved the modified opening configuration of insert #31 shown in figure 13. Since this result (#275) completed the optimization study, the results obtained in the former stages of the optimization study and the baseline wing results are included with test run #275 in figure 15. Relative to the results of test

run #266, the outboard modification opening geometry change increased the value of $C_{L_{max}}$ with an accompanying decrease in α_{stall} of 2 degrees.

Although the change in lift characteristics was the primary criteria used in the optimization study, the change in drag and pitching moment associated with the leading edge modifications were recorded for each test run. The drag and pitching moment characteristics of the configuration studied in test run #275 are representative of the results obtained with other modification configurations.

Figures 16 and 17 show the drag and pitching moment data of test run #275 relative to the baseline wing. From 0 to 19 degrees angle of attack the drag of the modified wing was slightly less than that of the basic wing.

The modified wing results showed a slight decrease in the stall (nose up pitching moment) gradient and a 7 degree angle of attack margin, for this pitch up, relative to the baseline wing.

The results of test runs #249, #266 and #275 show that an increase in $C_{L_{max}}$ is accompanied by a decrease in α_{stall} . Additionally, it was noted that the lift readings fluctuated significantly in the angle of attack range above 30 degrees during the test runs of the optimization study. The decrease in α_{stall} with increase in $C_{L_{max}}$ and fluctuating lift values were not experienced in the straight wing test program. Thus a study was conducted to identify the cause of these two phenomenon. The distance between the swept wing root leading edge and the upper surface of the wind tunnel was significantly decreased at the higher angles of attack. Thus it appeared plausible that this tunnel surface was interfering with the wing flow field at the higher

angles of attack. Wool tufts were attached to the ceiling of the tunnel to aid in obtaining some physical evidence of the flow field impinging on this surface. In subsequent wind tunnel tests these tufts showed a high activity level only when the lift values fluctuated. This correlation appeared to verify the existence of flow field interference associated with the leading edge modifications which developed high C_L values in the angle of attack range above 30 degrees. This interference appeared to prevent a stable development of the vortex flow field generated by the leading edge modification, resulting in a formulation/ dissipation cyclic process.

It was felt that the upper lift values obtained, in the angle of attack range above 30 degrees, probably represented the lift generated by a modified wing with a stable vortex flow field. Thus the averaged values recorded by the data acquisition system gave a conservative result of the modified wing's performance at these angles of attack. A leading edge modification configuration was tested which used the modified insert #30 at the 3A/ 3B location and the modified insert #26, shown in figure 13, at the 6A/ 6B location. This test configuration developed relatively large lift fluctuations above 30 degrees α and both high and low values were manually recorded. The results of this test are shown in figure 18.

The high value lift results are similar to those achieved in the straight wing tests where the leading edge of the wing did not come as close to the upper tunnel surface as the swept wing at these high angles of attack. These test data indicate that the modified swept wing results of this study may be conservative with regard to the $C_{L_{max}}$ and α_{stall} values.

3.2.3 Reynolds Number Study

A wind tunnel test speed of 39.62 m/sec was used for both the straight and swept wing model tests. This resulted in an average test Reynolds number of 1.3×10^6 for the tests conducted in this study.

Upon finishing the optimization study, a modification was rerun at a tunnel speed of 21.34 m/sec. The results were compared with those obtained with a tunnel speed of 39.62 m/sec to evaluate the significance of Reynolds number effects. A similar test series was conducted with the basic wing. These two comparisons are plotted in figure 19 as a difference value obtained between the higher and lower Reynolds number tests for each configuration.

The similarity between the two results indicates that the Reynolds number effect evidenced in the modified wing results is associated with the basic wing.

Structural considerations of the balance tripod attachment member precluded higher test speeds and Reynolds numbers with the wing models of this study.

3.3 Flow Visualization Study

In the exploratory study, a preliminary analysis of the modified flow field was conducted with wool tufts and smoke injection. In the swept wing test program fluorescent dye/oil smear tests were conducted to provide additional flow field information. Ultraviolet light was used to photograph the smear contours generated by the modification flow field. The results

of both straight and swept planform flow visualization tests were used to construct a model of the modified wing flow field.

These results indicated that the primary contribution of the leading edge openings is a pair of vortices generated at each side of the opening. These vortices extend downstream over the wing surface and influence the lift characteristics of the wing in two ways. Each rotational vortex flow field produces an incremental decrease in static pressure and induces a lower effective angle of attack on the wing surface outside the area lying behind the modification opening. An accompanying increase in effective angle of attack is induced in the area behind the modification opening. Since this area is confined between the pair of vortices, its influence is limited relative to the area experiencing the lower induced angle of attack. A more detailed description of how the vortices affect the wing lift characteristics is contained in reference 5. The sketch shown in figure 20 provides a pictorial representation of the modification opening flow field synthesized from the flow visualization tests conducted to date.

The fluorescent dye/oil smear tests were also used to obtain some physical interpretation of the swept wing force/moment characteristics. Figures 21 and 22 show the smear contours obtained with the one and two modification insert configurations. Significant aspects of the flow field indicated by each contour pattern is described below each photograph.

4. DISCUSSION OF RESULTS

The straight wing tests were conducted to provide information on the relationships between specific features of the modification opening geometry and their associated lift characteristics.

Additional testing will be needed to identify the optimization criteria for the modification chordwise opening size. The teardrop modification opening study indicated that proper tailoring of the modification opening shape can be used to reduce the drag of the modified wing in the low angle of attack regime. These drag results actually showed a slight improvement in drag compared to the basic wing from 4 to 11 degrees angle of attack.

The swept wing force/moment results were achieved by a parametric study of location and modification geometry variables. The stall angle of attack has been increased from 27 degrees (basic wing) to 36 and 34 degrees with the modifications of test runs #266 and #275, respectively. A maximum lift coefficient comparable to the basic wing was achieved by the modification configuration of test run #275. The wind tunnel interference study results indicate that the potential of the leading edge modification to increase the stall angle of attack and lift coefficient relative to the basic wing can be significantly greater than the results obtained in test runs #266 and #275.

The drag and pitching moment characteristics obtained in test run #275 were representative of those obtained with the other modification configurations. The modification results showed no increase in drag below 19 degrees and a small improvement in the stall nose up pitching moment

relative to the basic wing. No attempt was made to modify or improve the drag or pitching moment characteristics obtained with the leading edge modification openings. Thus more improvement in these characteristics could be expected with proper geometry tailoring of the leading edge openings.

The results of the fluorescent dye/oil smear tests conducted on the swept wing correlated with the tuft and smoke tests performed previously with the straight wing in identifying the primary features of the modification flow field. These tests indicated that a vortex was formed on either side of the modification opening. The flow field of these vortices induced a higher angle of attack on the wing area lying downstream of the opening and a lower angle of attack on either side of this region downstream of the opening.

The velocity of the vortex flow field produced an additional reduction in static pressure compared to the unmodified wing flow field. This lower static pressure produced an additional suction on the wing surface underlying each of the vortices. This vortex lift and the lower induced angle of attack appear to be the mechanism by which the modification opening changes the lift, drag and pitching moment of a modified wing.

It should also be stressed that these results do not represent the optimum leading edge configuration. The scope of this study did not allow a thorough optimization program to be completed.

This study also served to identify other enhancing characteristics associated with the leading edge modifications:

1. The lift versus angle of attack curve can be tailored with changes in the modification geometry.
2. The modifications are passive and thus do not increase the pilot workload or fail to operate when neglected by the pilot.
3. The modifications are applicable to control surfaces which could further enhance an airplane's resistance to departure from controlled flight.

CONCLUSIONS AND RECOMMENDATIONS

On the basis of the experimental results given in this report, it is concluded that the leading edge modifications have the potential for increasing the lift capability and stall angle of attack and moderating the nose up pitching moment at stall. It is further concluded that these characteristics can serve to enhance: (1) aircraft maneuverability for the fighter and attack mission, and (2) aircraft stall resistance in the approach and landing phase of flight operations. Additionally, the test results indicate that these enhancing characteristics can be achieved with no increase in drag for the cruise and climb angle of attack range.

In addition to the above general conclusions, the following specific conclusions were also formulated.

1. The teardrop shape modification produced a lower drag coefficient relative to the elliptical shape modification when tested in the straight planform wing.
2. The chordwise modification opening study results did not define a trend for achieving an optimum opening dimension in the straight planform wing tests.
3. The swept wing tests showed that the leading edge openings increased the stall angle of attack from 27 to 36 degrees.
4. The swept wing tests showed that the lift obtained with the modification openings was increased when using two openings instead of one; the lift achieved with the two modification

- opening was comparable to that of the unmodified wing even with flow field interference present.
5. The wind tunnel interference study results indicated that the modification optimization results were adversely affected by the impingement of the modification flow field on the upper tunnel surface.
 6. The preliminary Reynolds number study results showed that in the range from $.8 \times 10^6$ to 1.4×10^6 no Reynolds number effects were associated with the leading edge modifications.
 7. The flow visualization study results correlated with the results of the exploratory study in indicating that the primary feature of the leading edge modification flow field was the pair of vortices generated at each side of the modification opening.

On the basis of the above conclusions, it is recommended that the leading edge modification study be extended into the free flight phase of development. This would involve conducting the wind tunnel tests and analytic studies needed to support the flight test program. The flight test vehicle could be a RPV, drone or manned aircraft; the manned aircraft would enable a more complete flight evaluation to be conducted and thus would be the preferred test vehicle. The flight test program would aid in defining the primary role which the leading edge modifications should be designed to perform.

REFERENCES

1. Kroeger, R. A. and Feistel, T. W., "Reduction of Stall-Spin Entry Tendencies Through Wing Aerodynamic Design," SAE Paper 760481, April 1976.
2. Feistel, T. W. and Anderson, S. G., "A Method for Localizing Wing Flow Separation at Stall to Alleviate Spin Entry Tendencies," AIAA Paper 78-1476.
3. Pankhurst, R. C. and Holder, D. W., "Wind Tunnel Techniques," Isaac Pitman and Sons, Ltd., London, 1952.
4. Pope, Alan and Harper, J. J., "Low-Speed Wind Tunnel Testing," John Wiley and Sons, Inc., 1966.
5. Sament, S. S., White, R. P. and Janakiram, D. S., "Summary of Theoretical and Experimental Investigations of Vortex Lift at High Angles of Attack," Report ONR-CR 212-223-5F, March 1979.

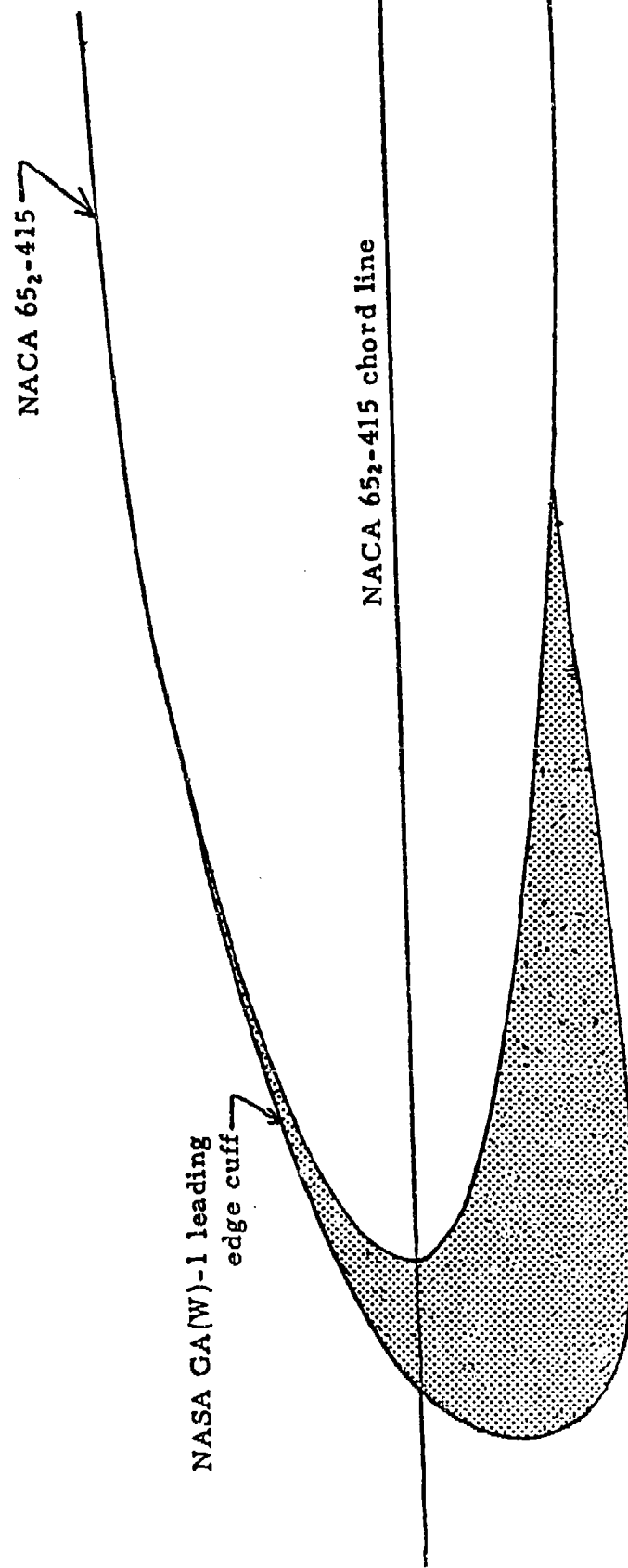


Figure 1. Airfoil Section of Straight and Swept Wing Wind Tunnel Models

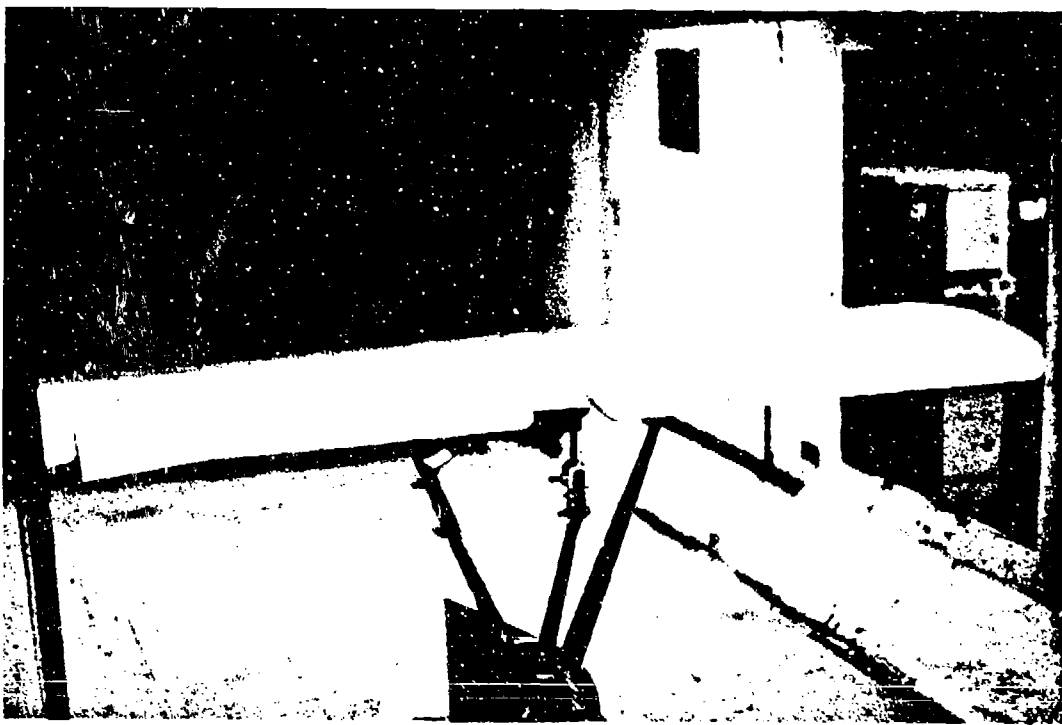


Figure 2. Straight Planform Wing Model Mounted on the Wind Tunnel Balance Tripod Support

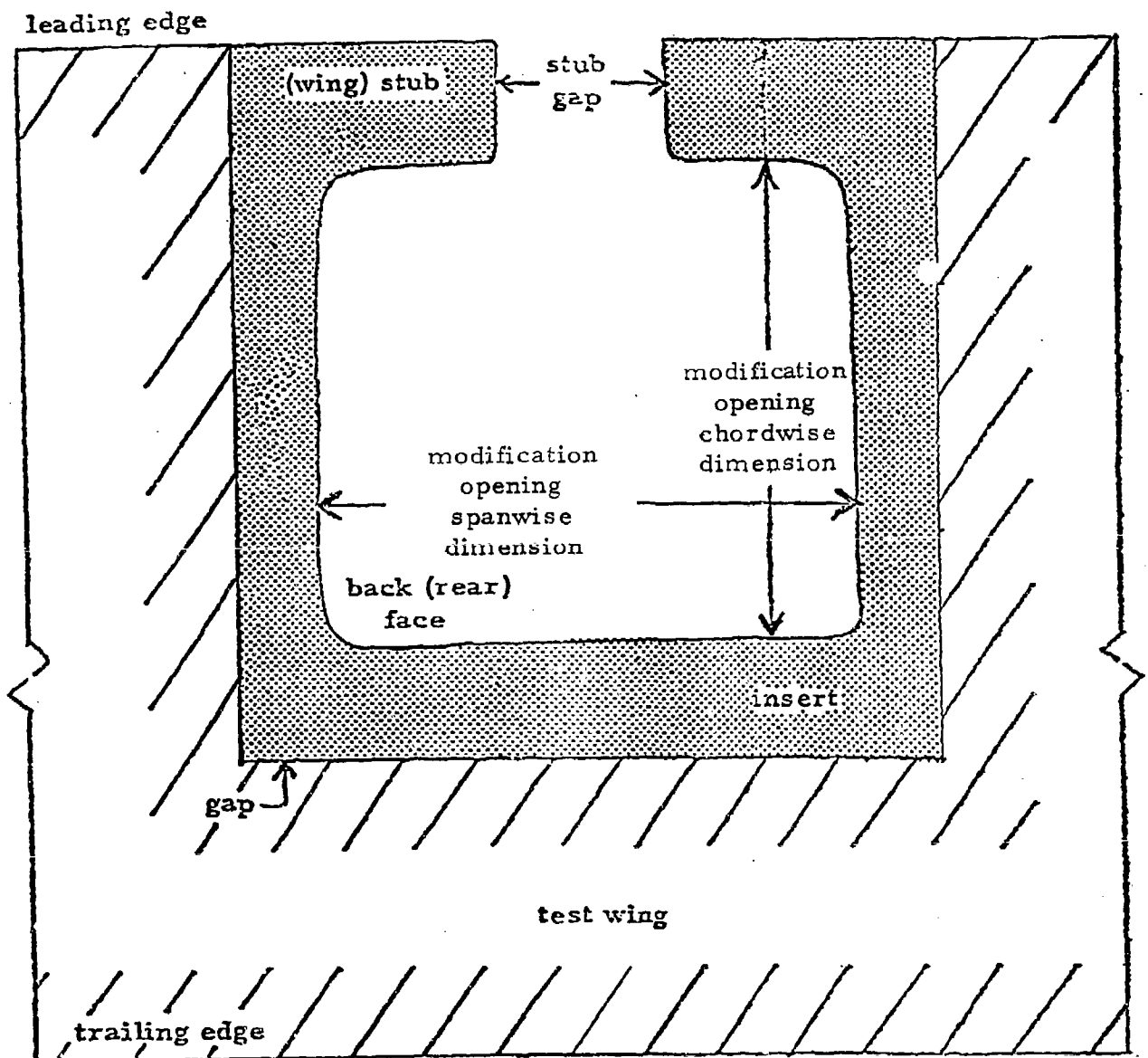
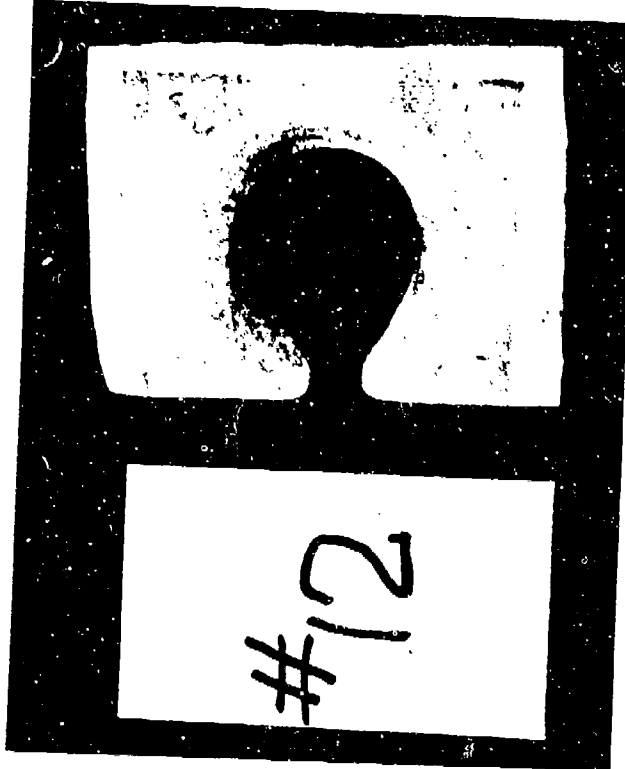


Figure 3. Nomenclature for Geometry Features of Leading Edge Modification Inserts



(a)



(b)

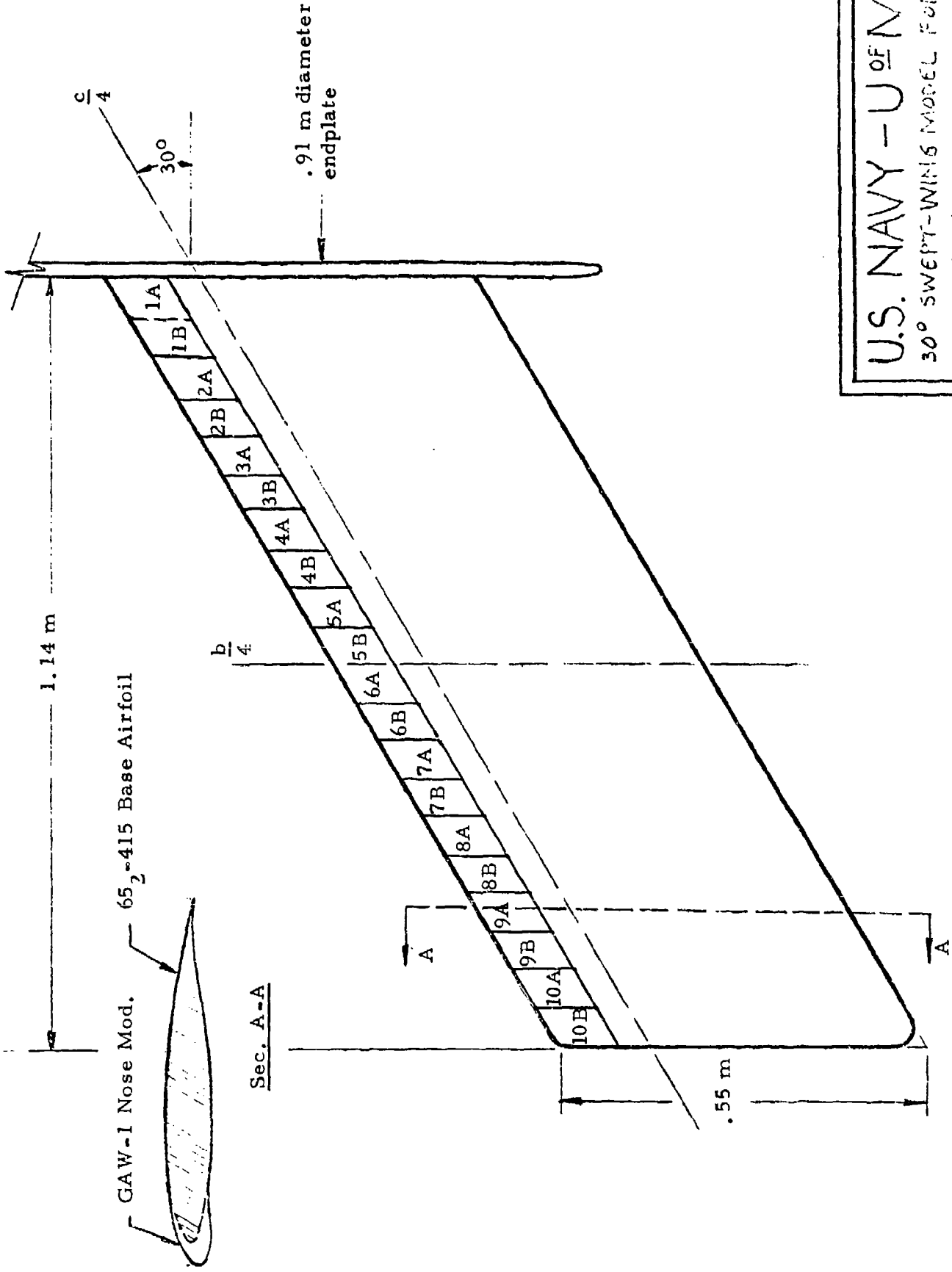


(c)



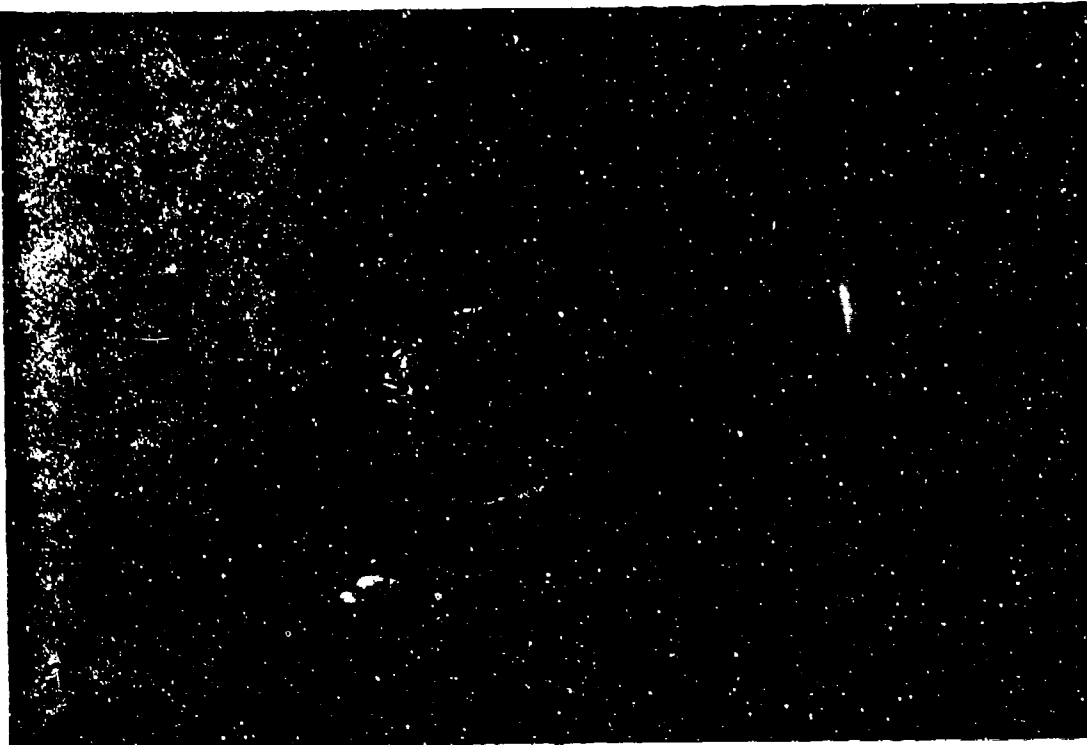
(d)

Figure 4. Leading Edge Inserts Used in the Straight Planform Wing Study with their Respective Modification Openings.



U.S. NAVY - U OF M
 30° SWEEP-WING MODEL FOR
 U-M 5' x 7' WINDTUNNEL
 SCALE: 1 to 8 DATE: 6/26/64

Figure 5. A Sketch of the 30 Degree Sweepback Wing with the Leading Edge Insert Station Designation



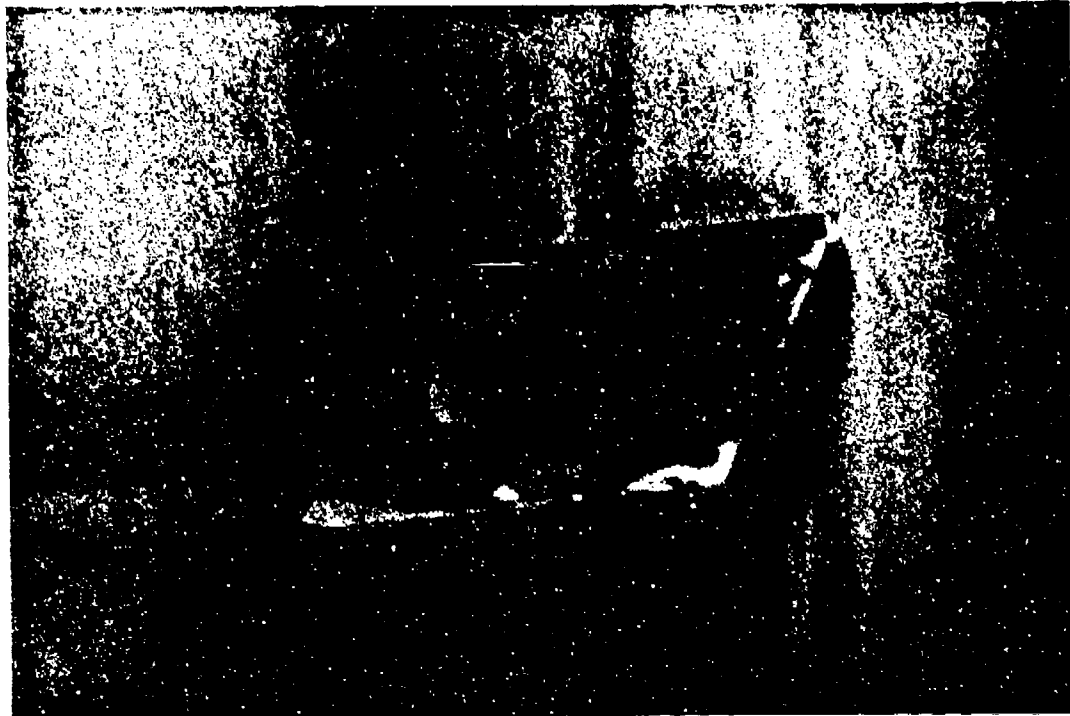
Insert #25

The dimensions of the primary geometrical features are given below:

1. Elliptical shape opening with the back face surface perpendicular to the wing tunnel longitudinal axis
2. Outboard stub thickness - 1.12 cm
3. Inboard stub thickness - 1.63 cm
4. Spanwise opening - 6.35 cm
5. Chordwise opening - 3.43 cm
6. Wing stub opening - 2.34 cm*

*Initial wing stub gap of insert #25 was .84 cm, the 2.34 cm opening shown above was made for a test examining the effect of increased gap size.

Figure 6(a). Leading Edge Inserts Used in the Swept Planform Wing Study with their Respective Modification Openings

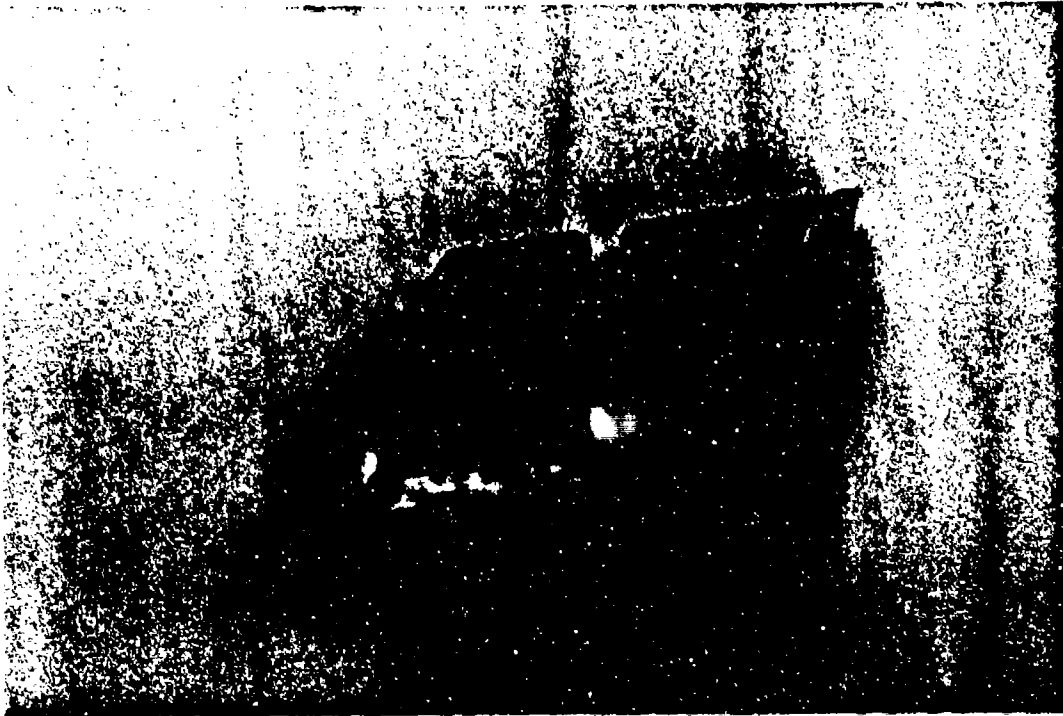


Insert #26

The dimensions of the primary geometrical features are given below:

1. Elliptical shape opening with the back face surface parallel to the wing leading edge
2. Outboard stub thickness - 1.14 cm
3. Inboard stub thickness - 1.40 cm
4. Spanwise opening - 7.04 cm
5. Chordwise opening - 3.38 cm
6. Stub gap opening - 0.79 cm

Figure 6(b). Leading Edge Inserts Used in the Swept Planform Wing Study with their Respective Modification Openings



Insert #30

The dimensions of the primary geometrical features are given below.

1. Teardrop shape opening
2. Outboard stub thickness - 1.35 cm
3. Inboard stub thickness - 1.35 cm
4. Spanwise opening - 3.96 cm
5. Chordwise opening - 4.14 cm
6. Stub gap opening - 0.97 cm

Figure 6(c). Leading Edge Inserts Used in the Swept Planform Wing Study with their Respective Modification Openings



Insert #31

The dimensions of the primary geometrical features are given below:

1. Elliptical shape opening with the back face surface parallel to the wing leading edge
2. Outboard stub thickness - 1.63 cm
3. Inboard stub thickness - 2.01 cm
4. Spanwise opening - 7.87 cm
5. Chordwise opening - 3.96 cm
6. Wing stub gap opening - 0.53 cm

Figure 6(d). Leading Edge Inserts Used in the Swept Planform Wing Study with their Respective Modification Openings

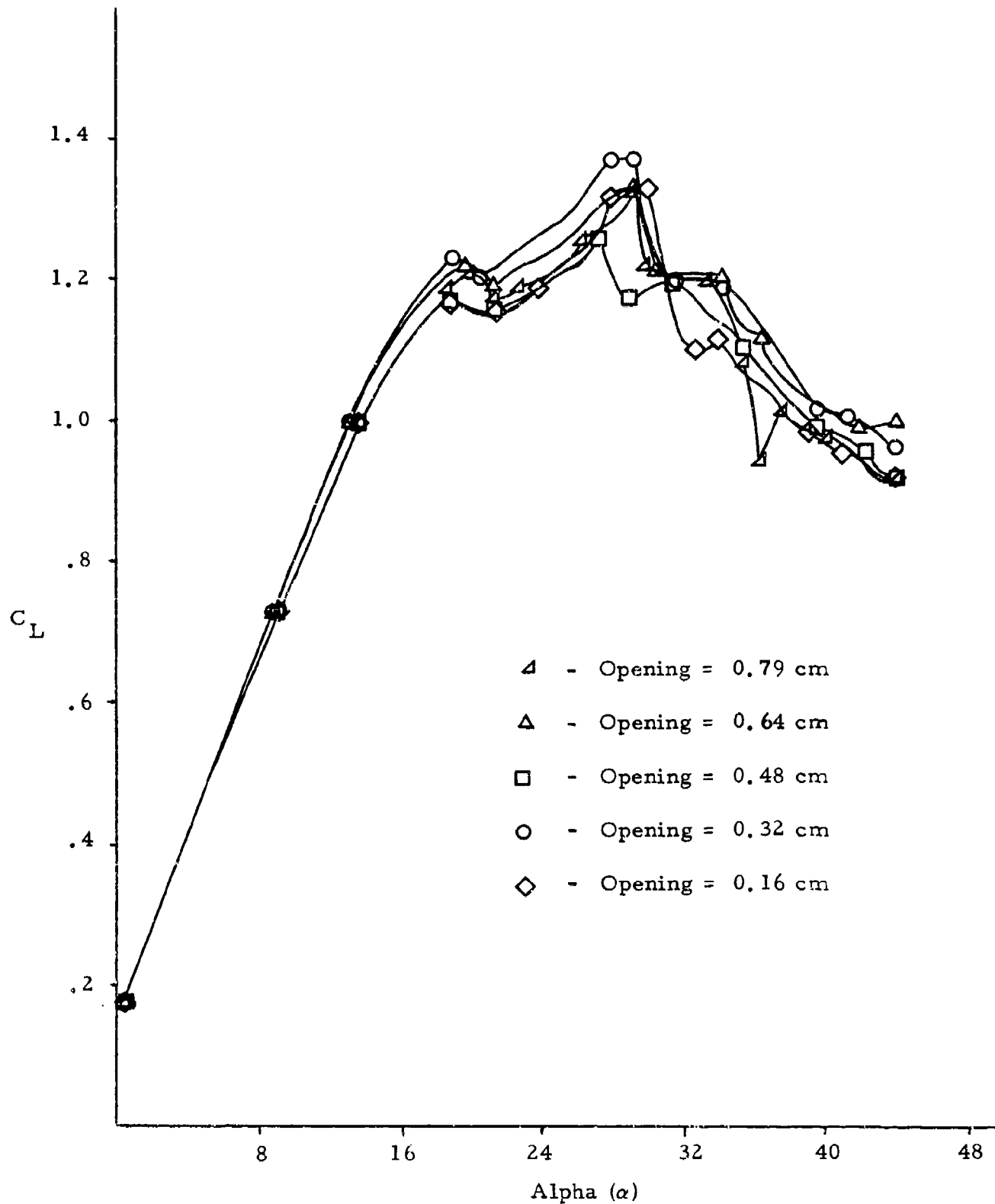


Figure 7. Lift Characteristics Associated with Varying Insert Cut-Out Chord Dimension

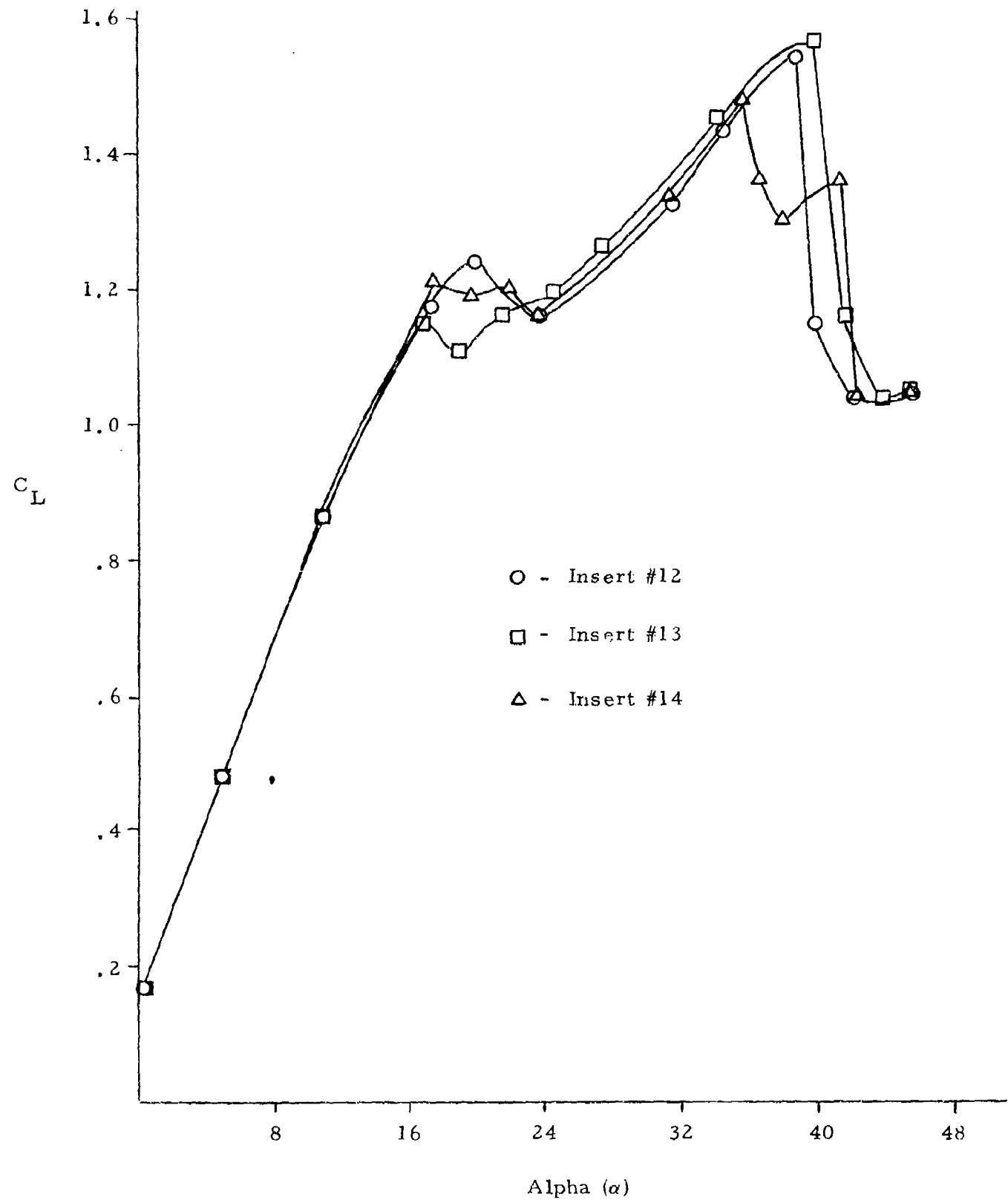


Figure 8. Lift Characteristics Associated with Three Teardrop Shape Modification Openings

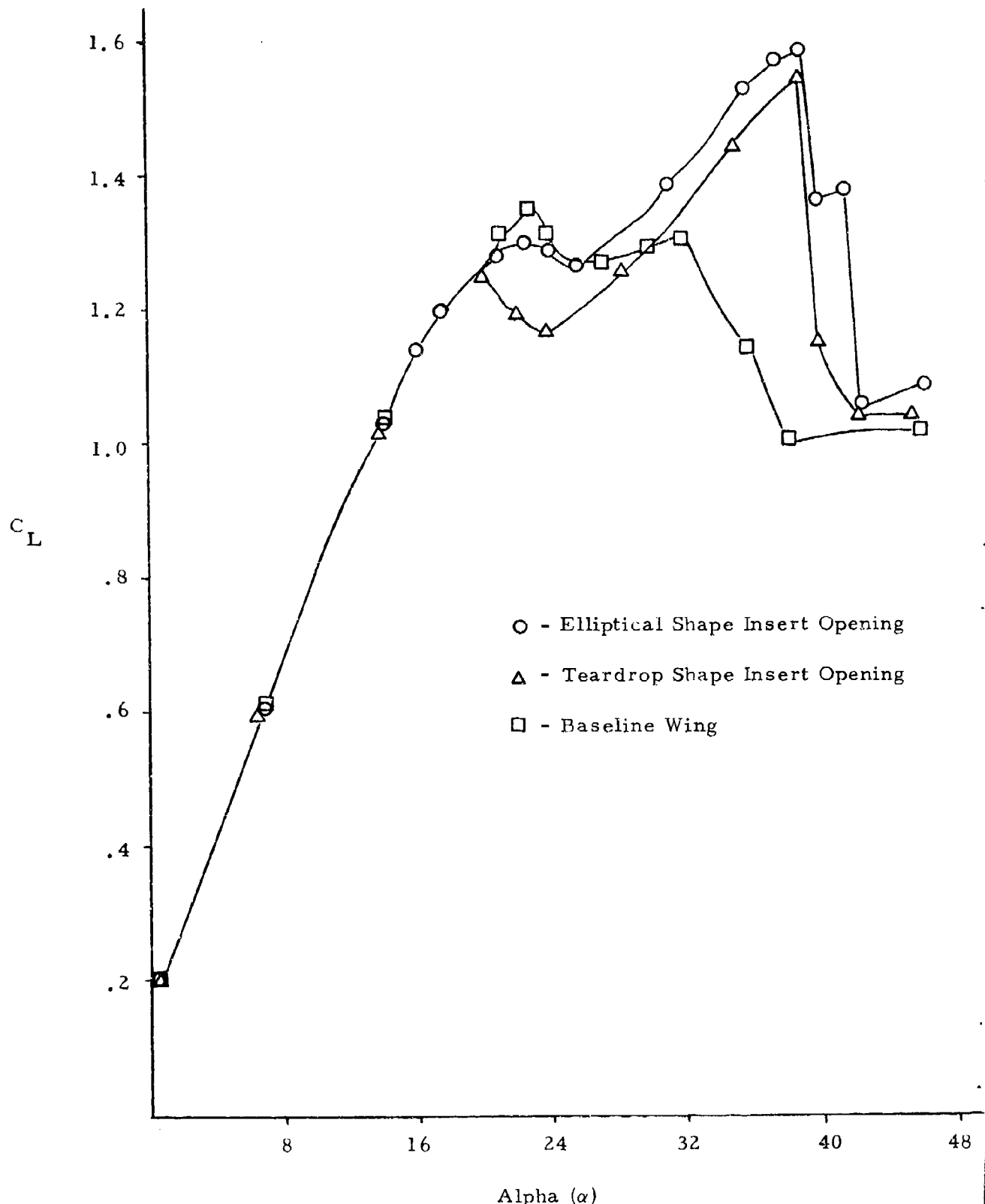


Figure 9. Lift Characteristics Associated with Teardrop and Elliptical Shape Insert Openings Compared with the Baseline Wing

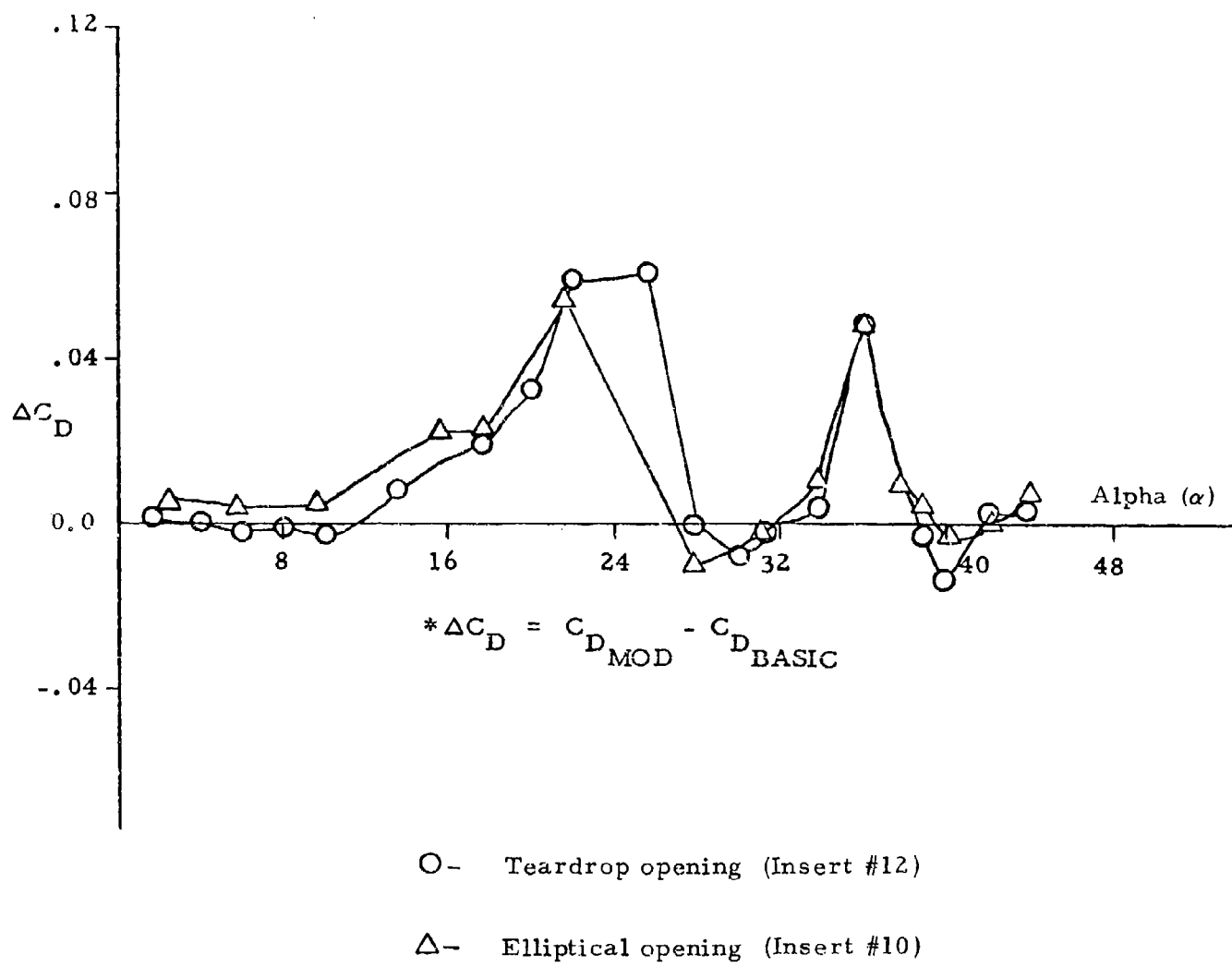


Figure 10. Comparison of Drag Characteristics Between Teardrop and Elliptical Shape Insert Openings

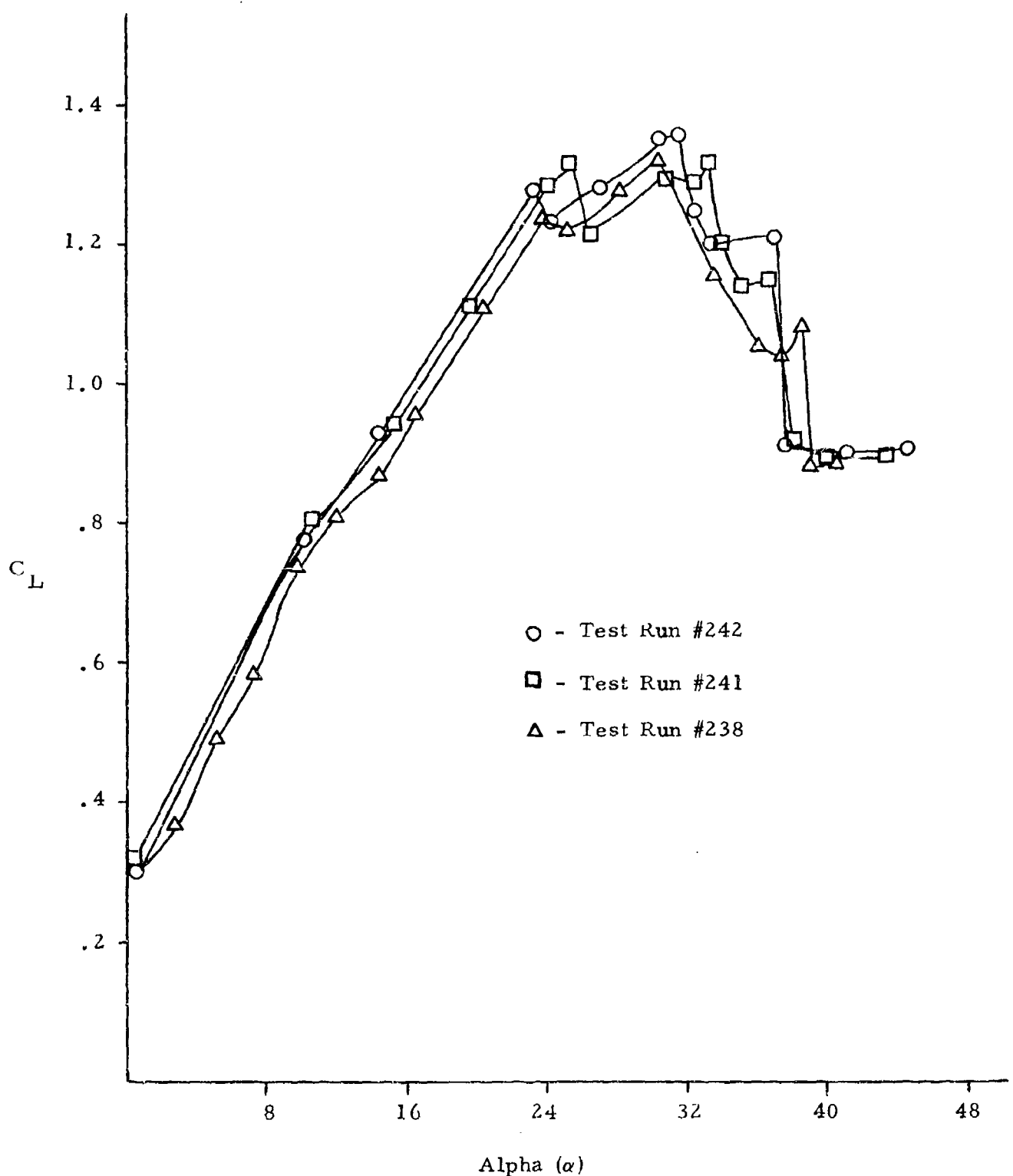


Figure 11. Preliminary C_L vs α Optimization Results Using One Modification Opening

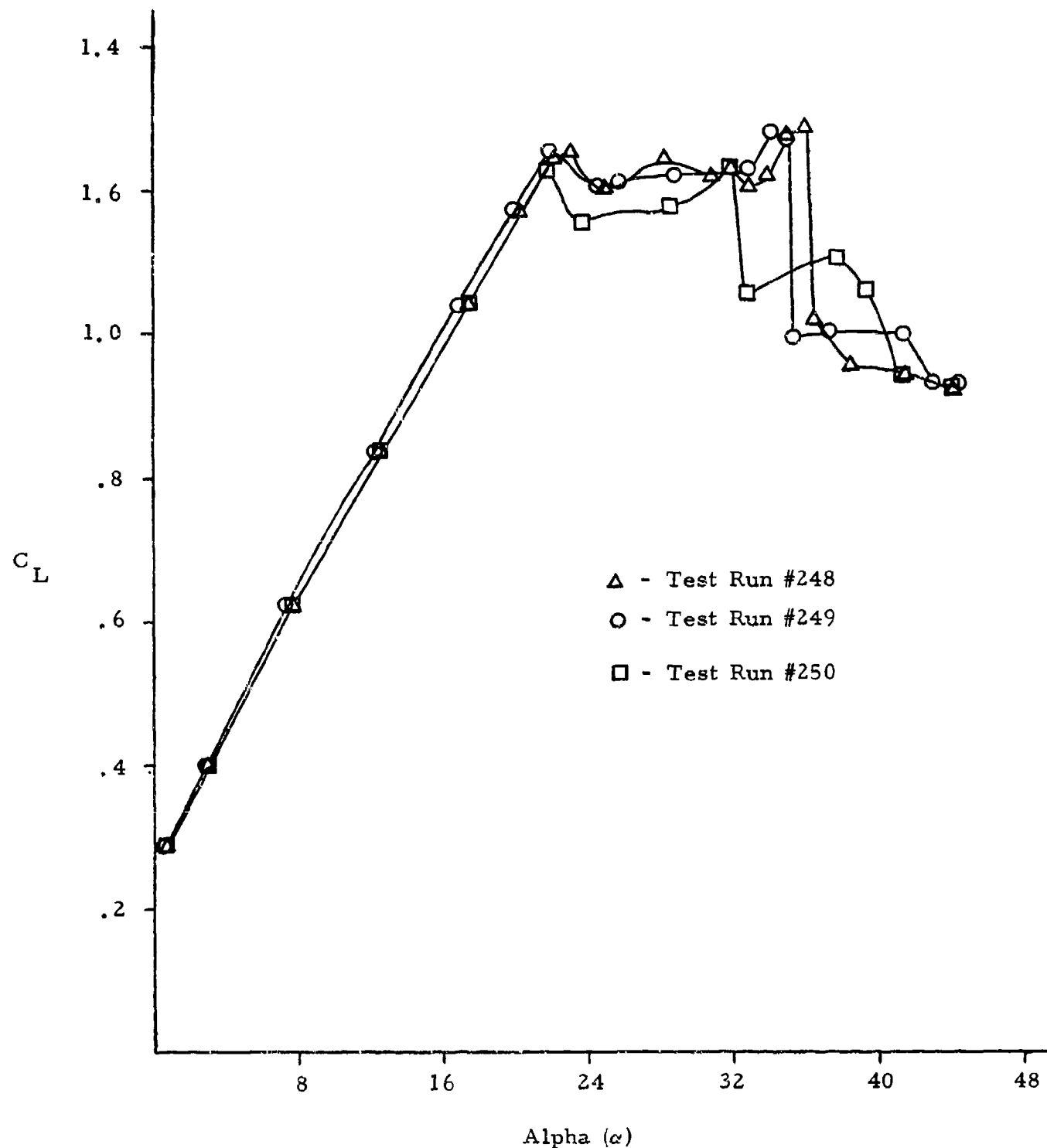
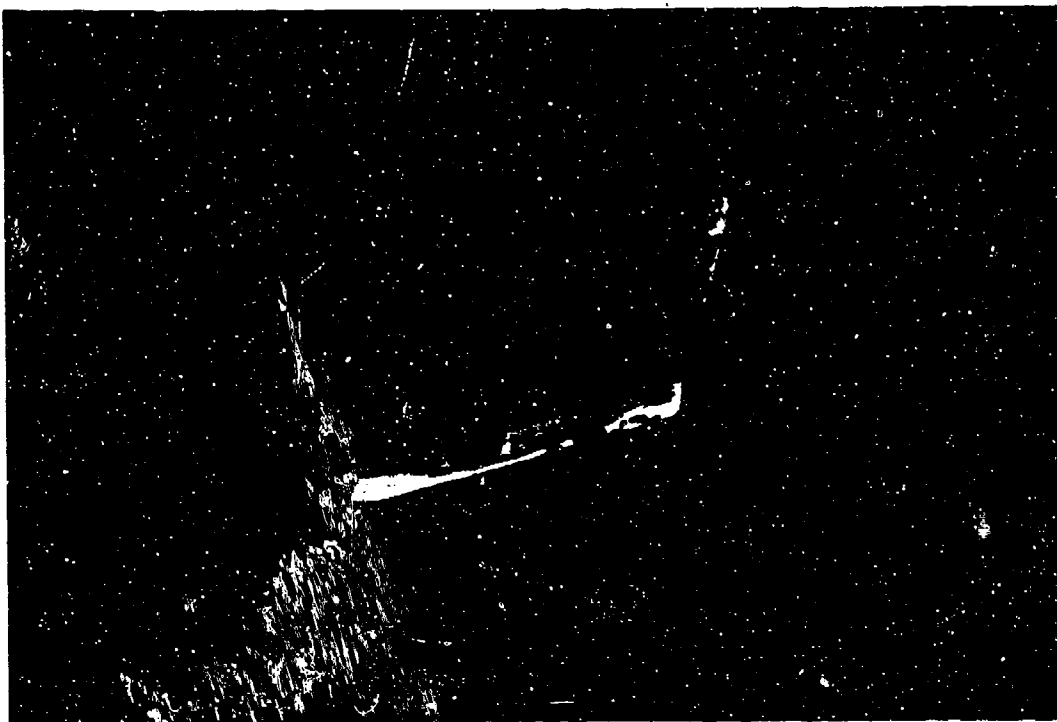


Figure 12. Preliminary C_L vs α Optimization Results Using Two Insert Openings

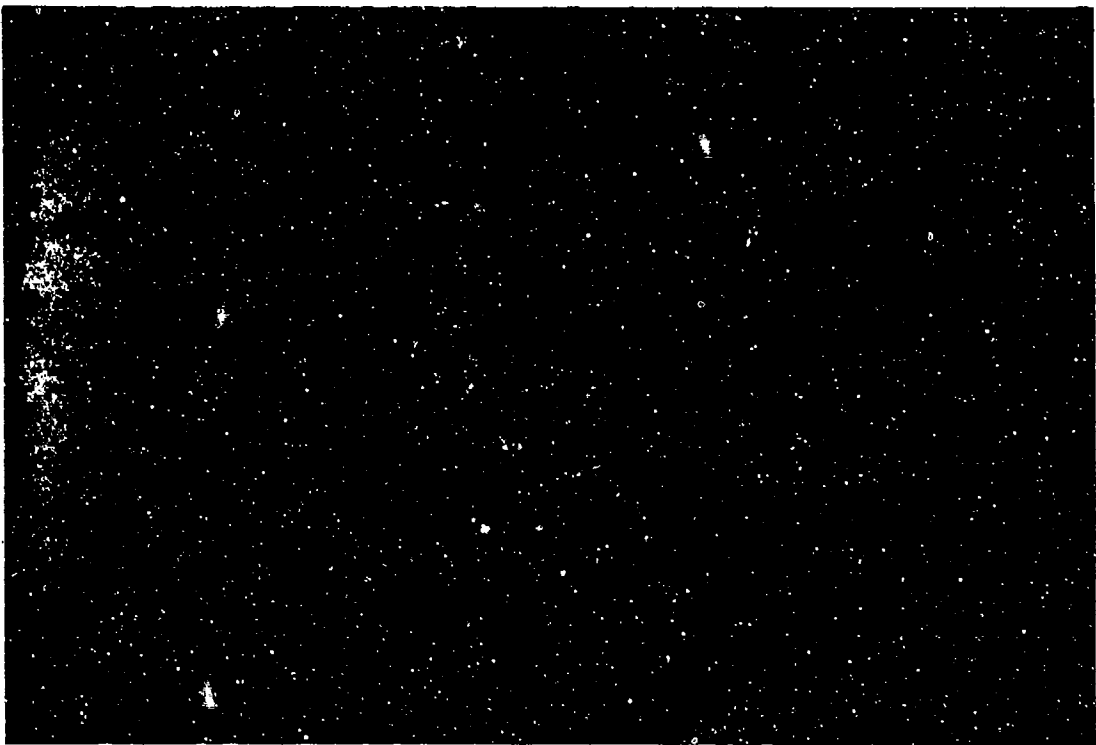


Insert #26 (Modified)

The dimensions of the primary geometrical features are given below:

1. Elliptical shape opening with the back face surface parallel to the wing leading edge.
2. Outboard stub thickness - 1.73 cm
3. Inboard stub thickness - 1.78 cm
4. Spanwise opening - 6.25 cm
5. Chordwise opening - 3.30 cm
6. Wing stub gap opening - 0.76 cm

Figure 13(a). Swept Wing Leading Edge Inserts with Modified Opening Geometry Developed in the Lift Optimization Study

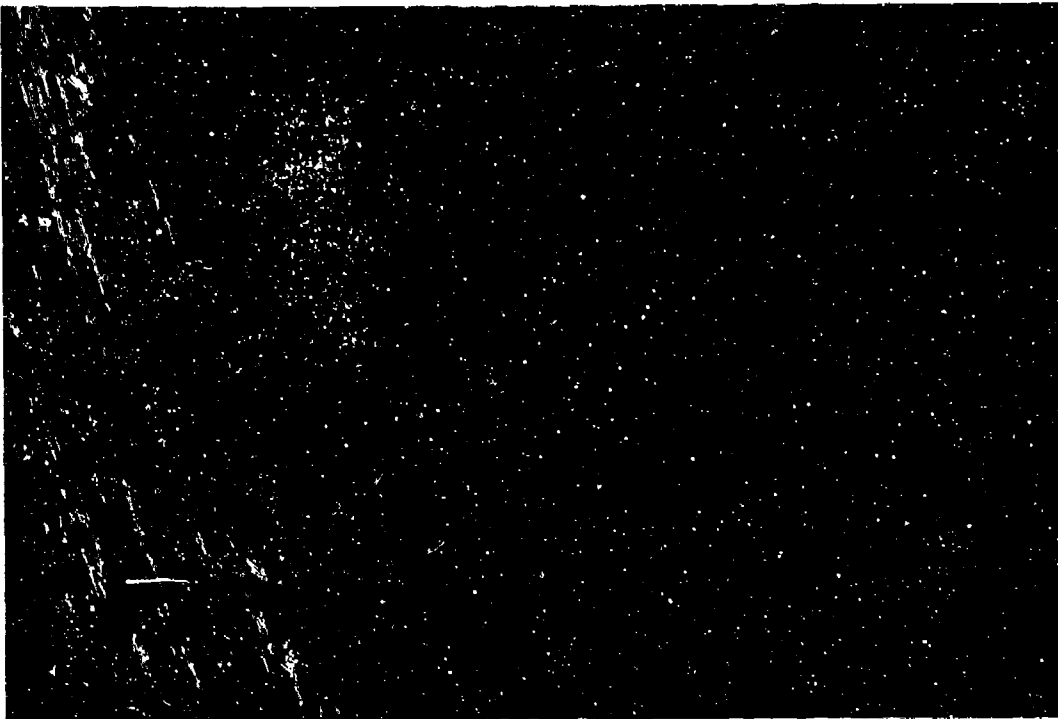


Insert #30 (Modified)

The dimensions of the primary geometrical features are given below:

1. Elliptical shape opening with the back face surface parallel to the wing leading edge
2. Spanwise opening - 1.07 cm
3. Chordwise opening - 0.61 cm

Figure 13(b). Swept Wing Leading Edge Inserts with Modified Opening Geometry Developed in the Lift Optimization Study



Insert #31 (Modified)

The dimensions of the primary geometrical features are given below:

1. Elliptical shape opening with the back face surface parallel to the wing leading edge
2. Outboard stub thickness - 2.44 cm
3. Inboard stub thickness - 1.91 cm
4. Spanwise opening - 6.73 cm
5. Chordwise opening - 3.63 cm
6. Wing stub gap opening - 1.09 cm

Figure 13(c), Swept Wing Leading Edge Inserts with Modified Opening Geometry Developed in the Lift Optimization Study

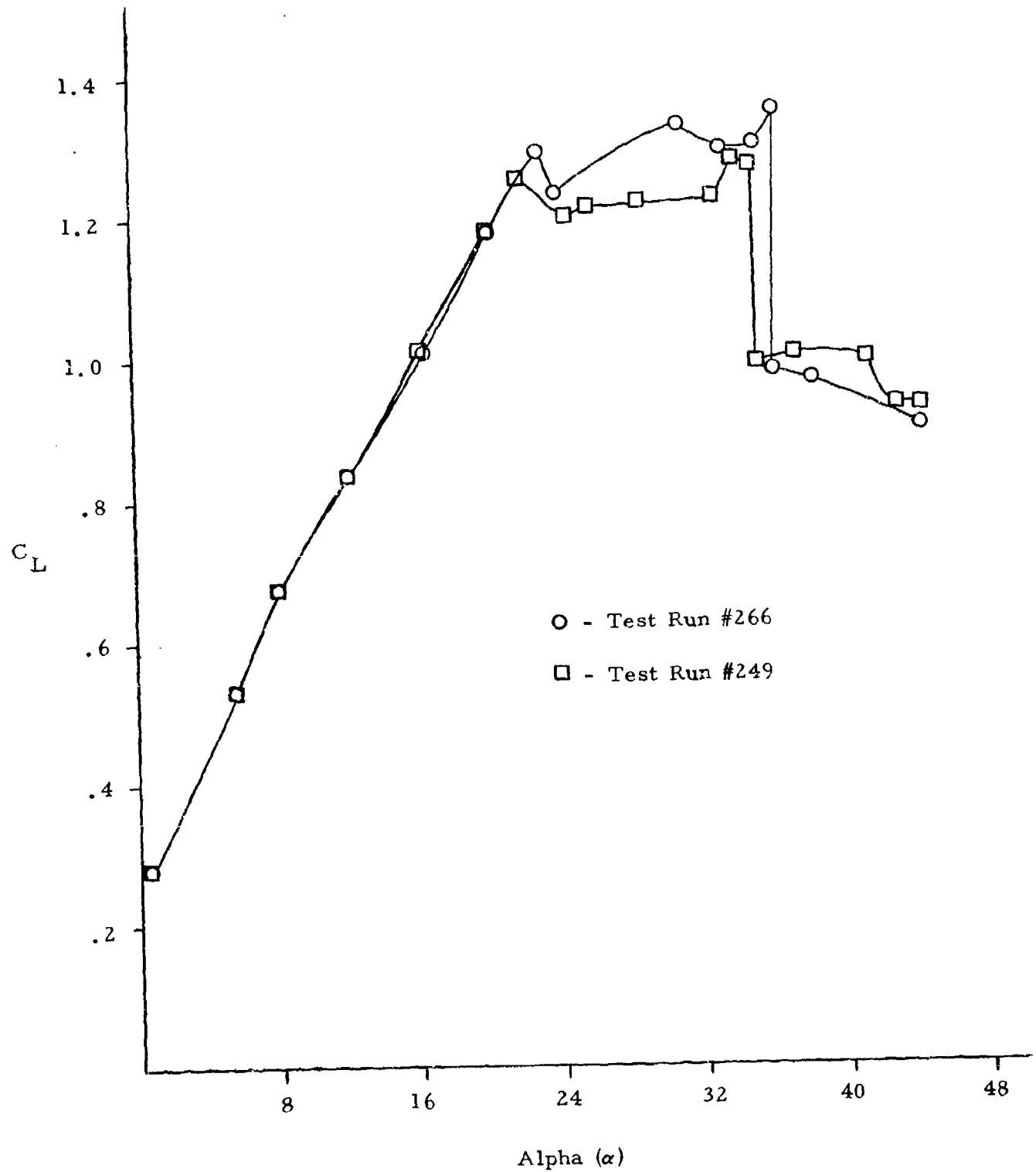


Figure 14. Lift Optimization Results Achieved by Changing the Inboard Insert Opening Geometry

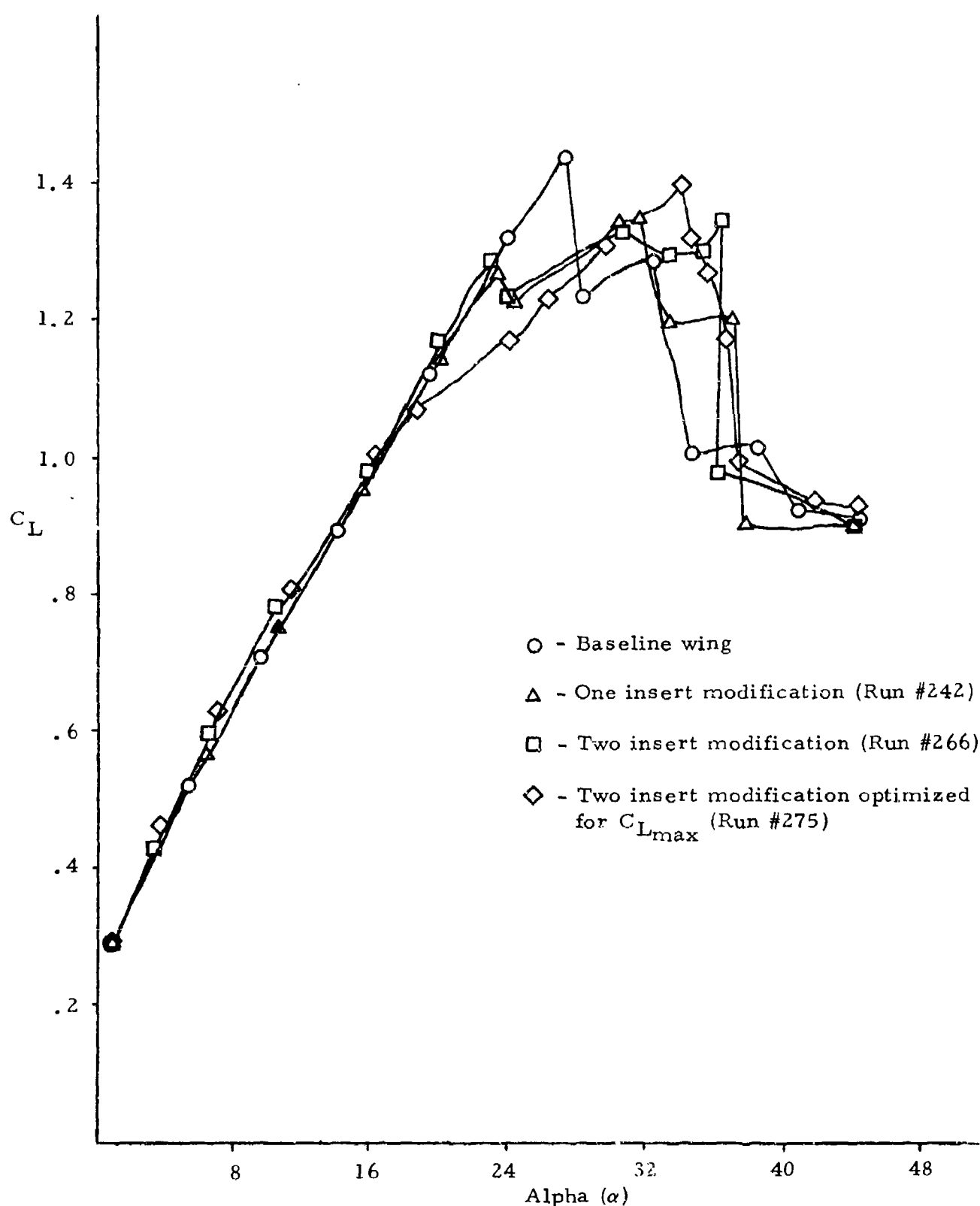


Figure 15. Lift Characteristics Achieved with Various Modification Insert Configurations During the Optimization of the Swept Planform Wing

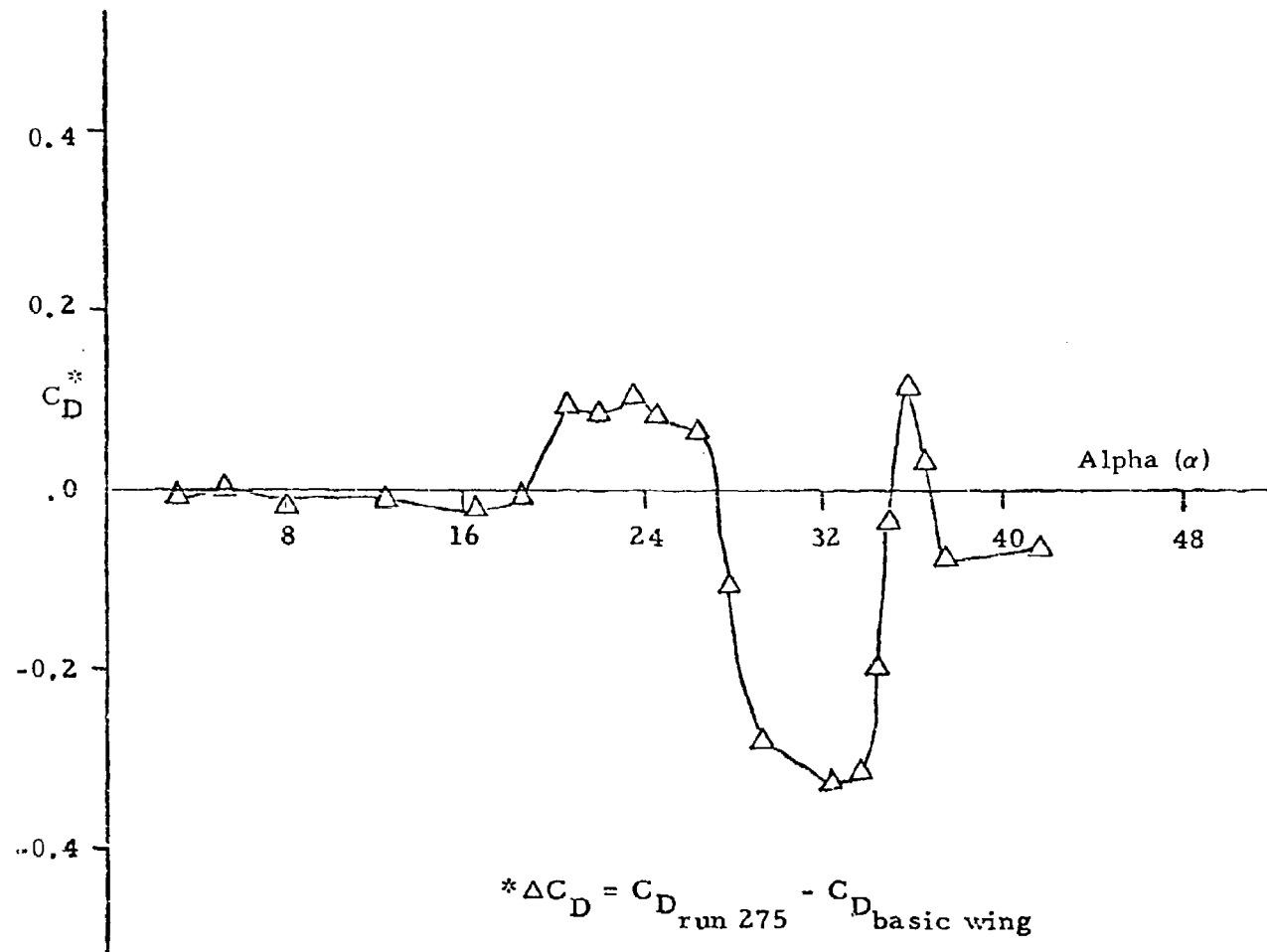


Figure 16. Change in Drag Associated with Leading Edge Modification Configuration of Test Run #275

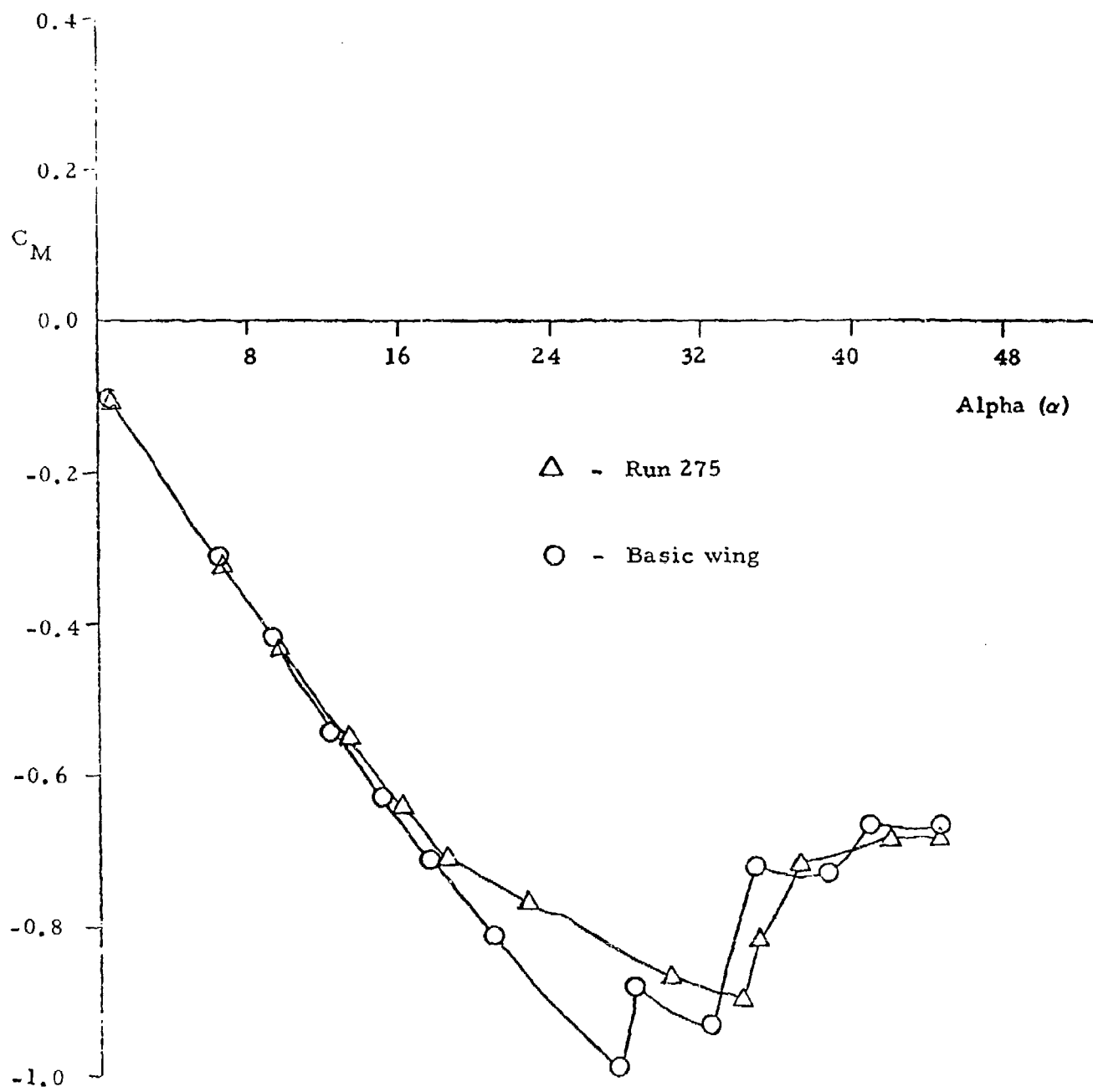


Figure 17. Comparison of the Pitching Moment Associated with the Leading Edge Modification Configuration of Test Run #275 with that of the Baseline Wing

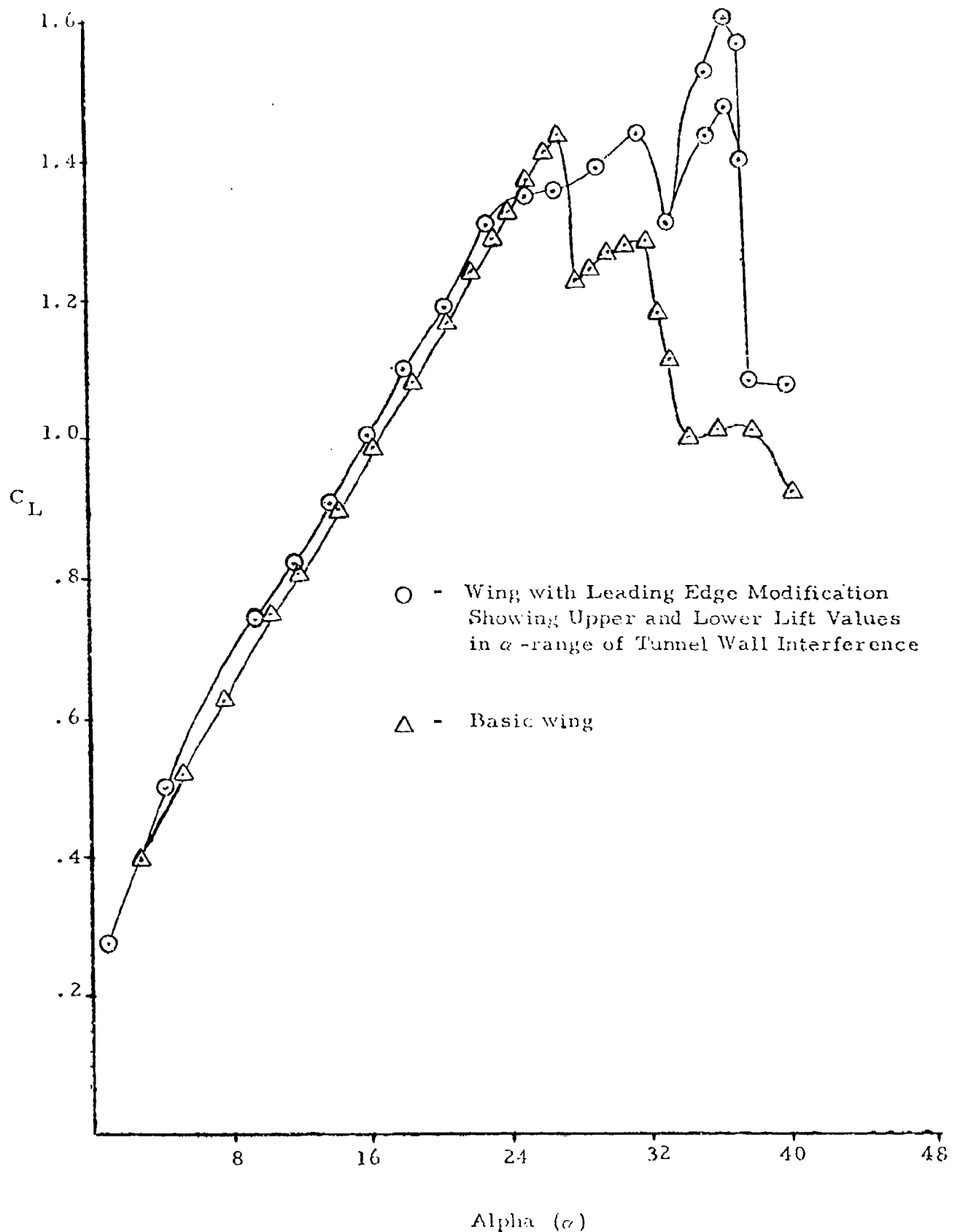


Figure 18. Comparison of Lift Characteristics between Modified and Basic 30° Swept Wing and Upper and Lower Lift Readings on the α -range of Tunnel Wall Interference

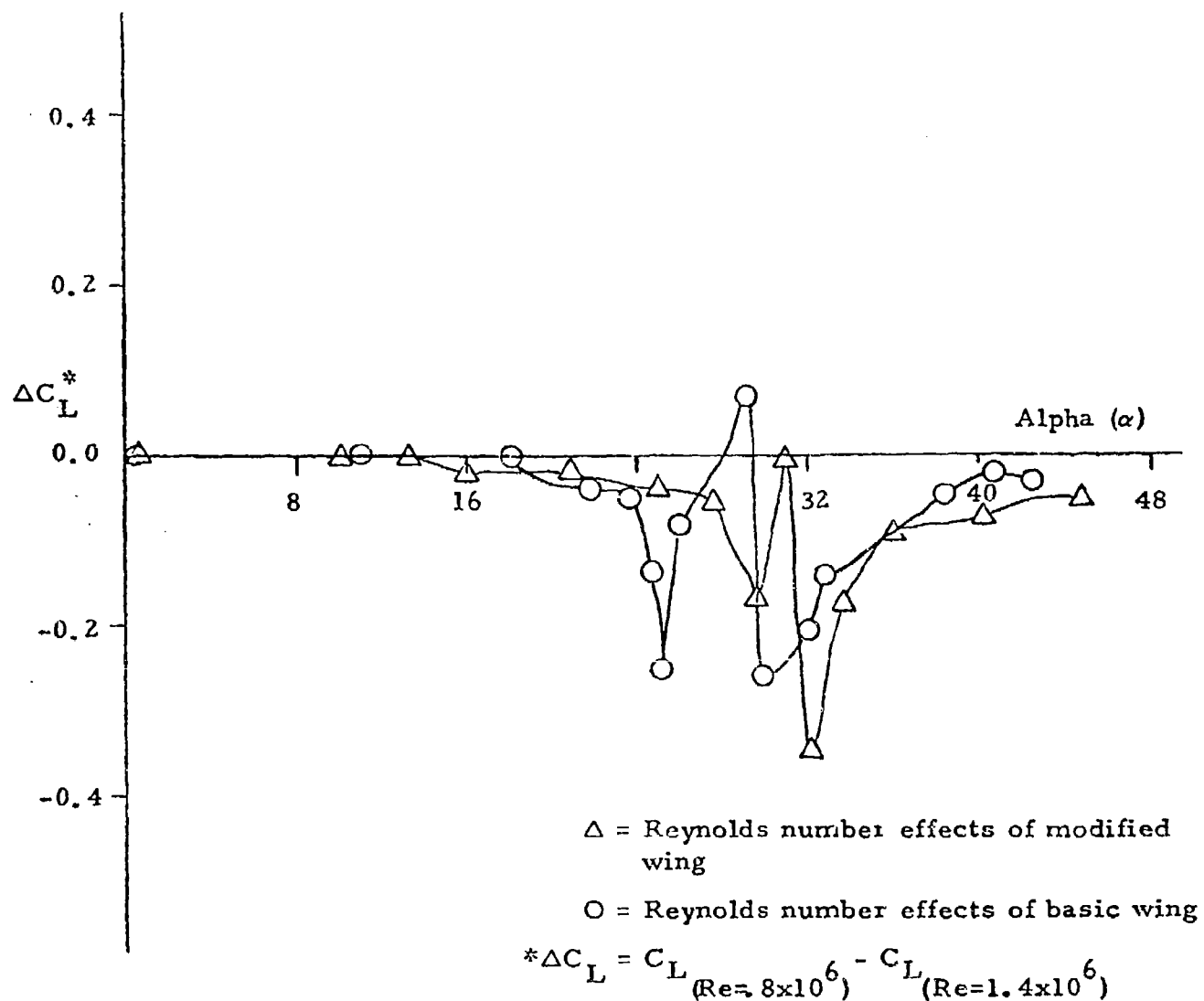


Figure 19. Comparison of Reynolds Number Effects Associated with the Modified and Baseline Swept Planform Wing

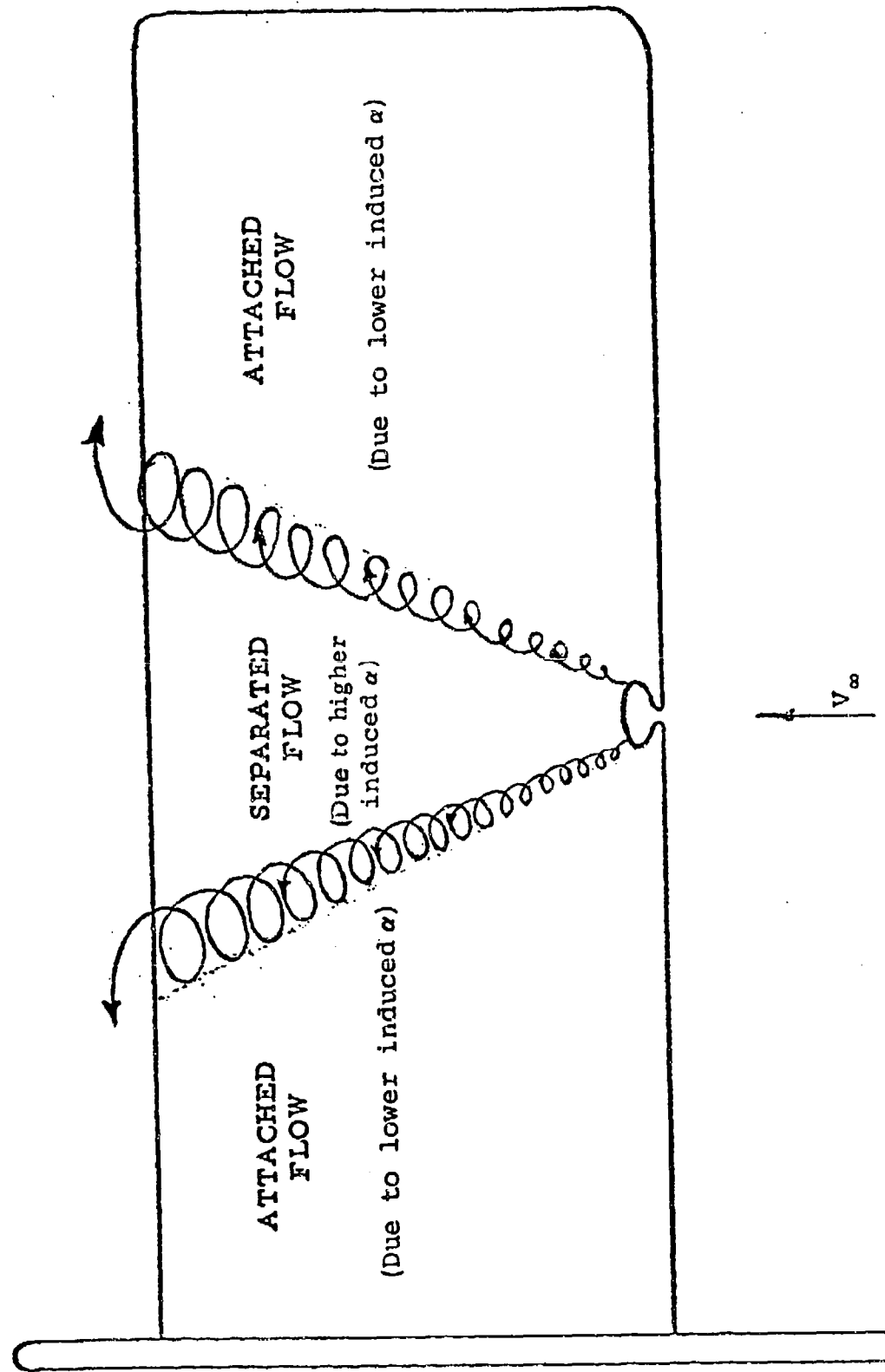
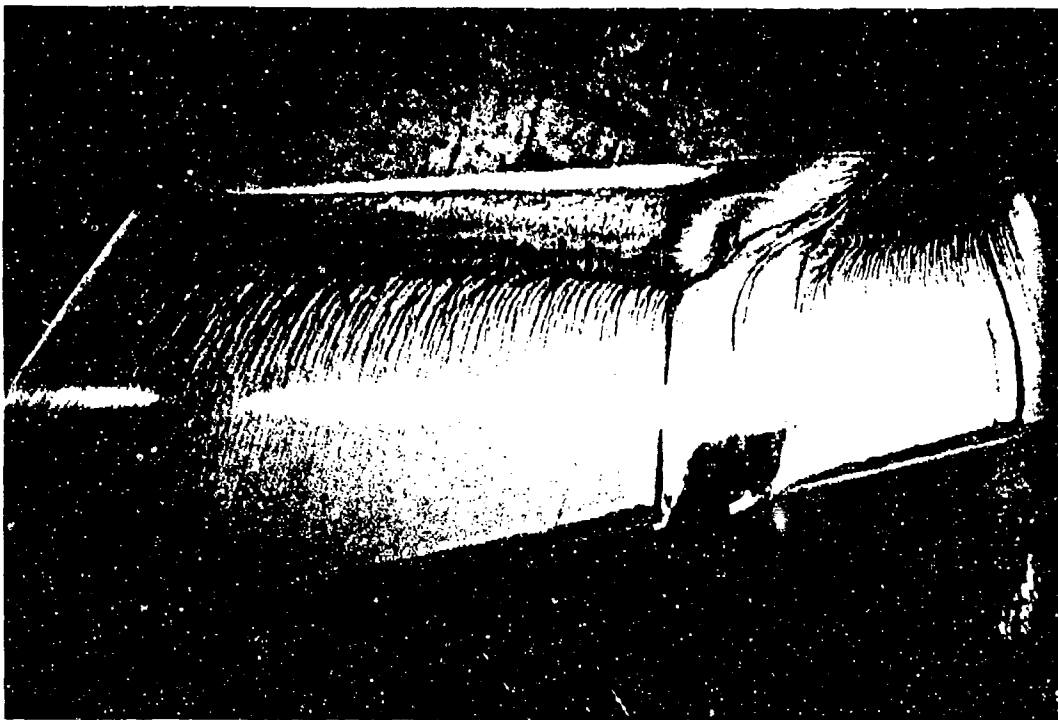


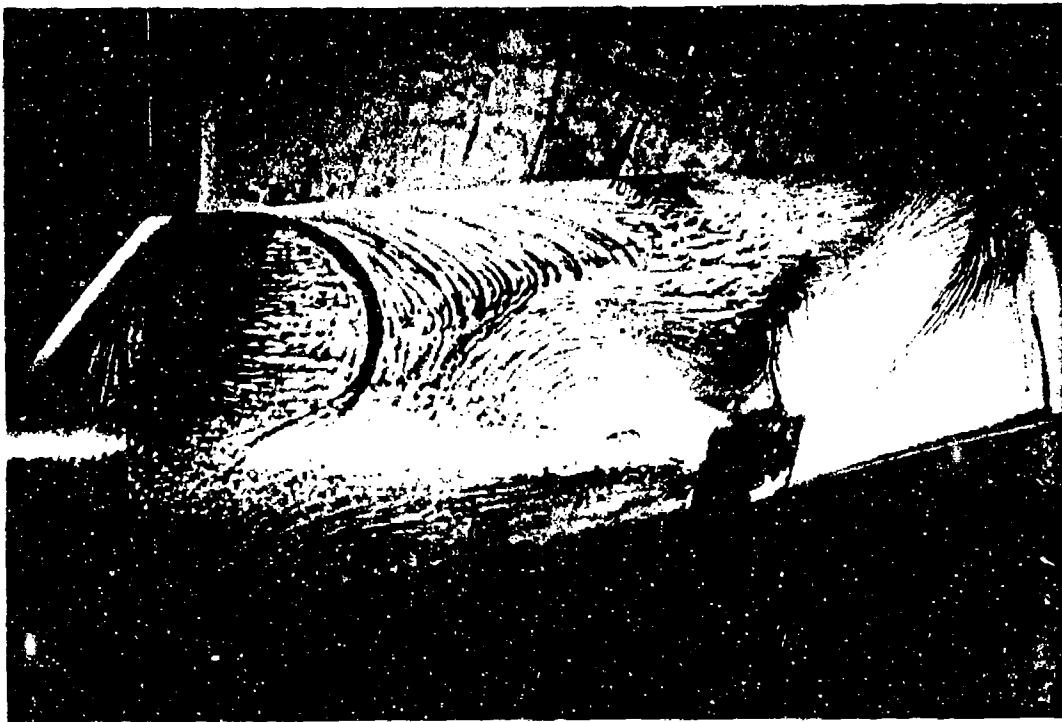
Figure 20. Sketch of the Representative Flow Field Associated with a Leading Edge Modification
Opening Located at the Wing Mid-Semispan Position



$$\alpha = 20^\circ, C_L = 1.11$$

This flow picture shows the smear profile being formed. The smear is being moved rearward, along the entire wing, from the leading edge to about 50 percent of the chord. Aft of this chord position no movement is seen, indicating that the flow has separated. The two paths extending rearward from each side of the modification opening are the areas experiencing the maximum decrease in induced angle of attack from the vortex flow fields. The vortices have formed on each side of the modification opening and extend rearward parallel with the wing flow field streamlines.

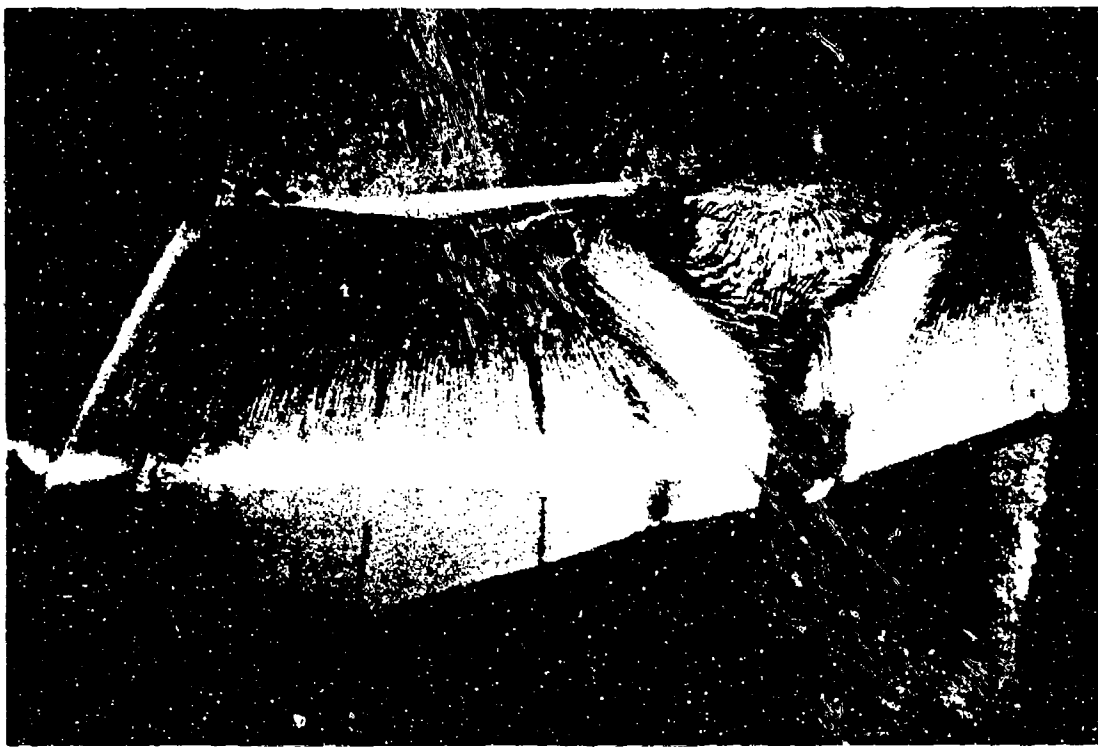
Figure 21(a). Fluorescent Dye/Oil Smear Contours Associated with One Leading Edge Insert Opening



$$\alpha = 25^\circ, C_L = 1.28$$

The smear profile at 25 degrees angle of attack shows that reverse flow exists at the inboard trailing edge area. This reverse flow develops a circular flow field which dominates a large area of the inboard wing section. It also appears to have influenced the inboard vortex since the axis of this vortex is rotated closer to the leading edge than is normally observed. The axis of the outboard vortex passes roughly over the wing tip trailing edge.

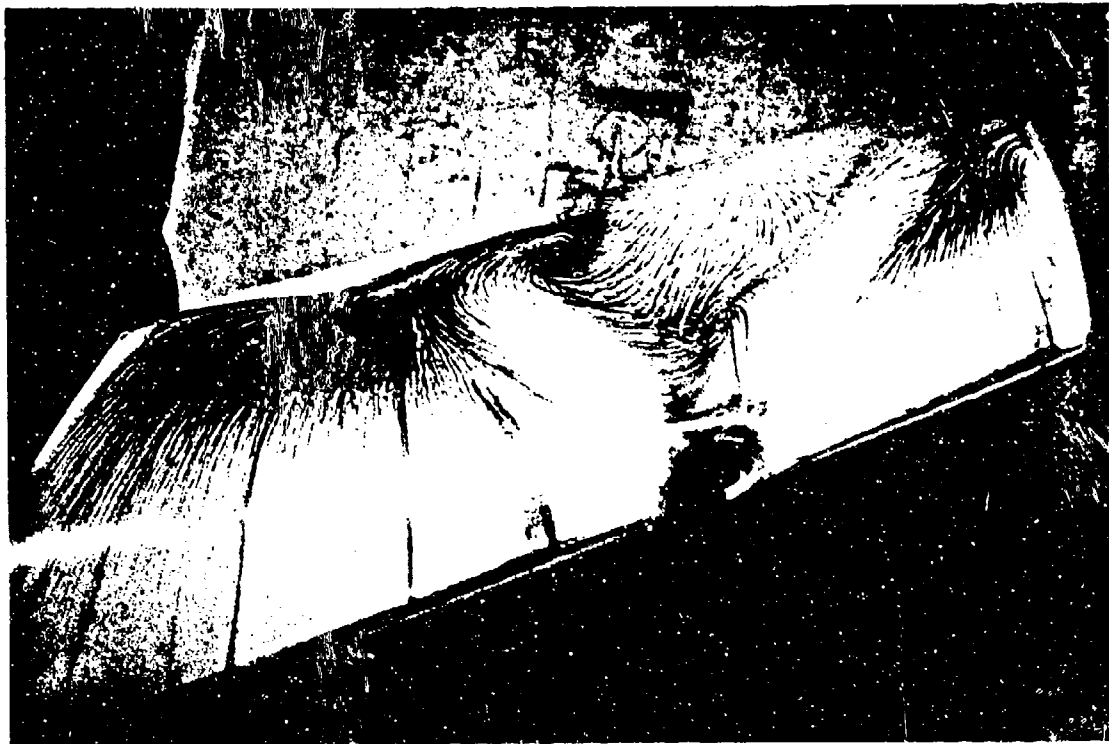
Figure 21(b). Fluorescent Dye/Oil Smear Contours Associated with One Leading Edge Insert Opening



$$\alpha = 33^\circ, C_L = 1.30$$

This flow pattern picture shows the two vortex axes extending rearward from the modification opening. The angle between the vortex axes is typical for this angle of attack. Separation areas exist between the axes of the vortex and on the inboard aft wing section. Spanwise flow exists along the inboard trailing edge.

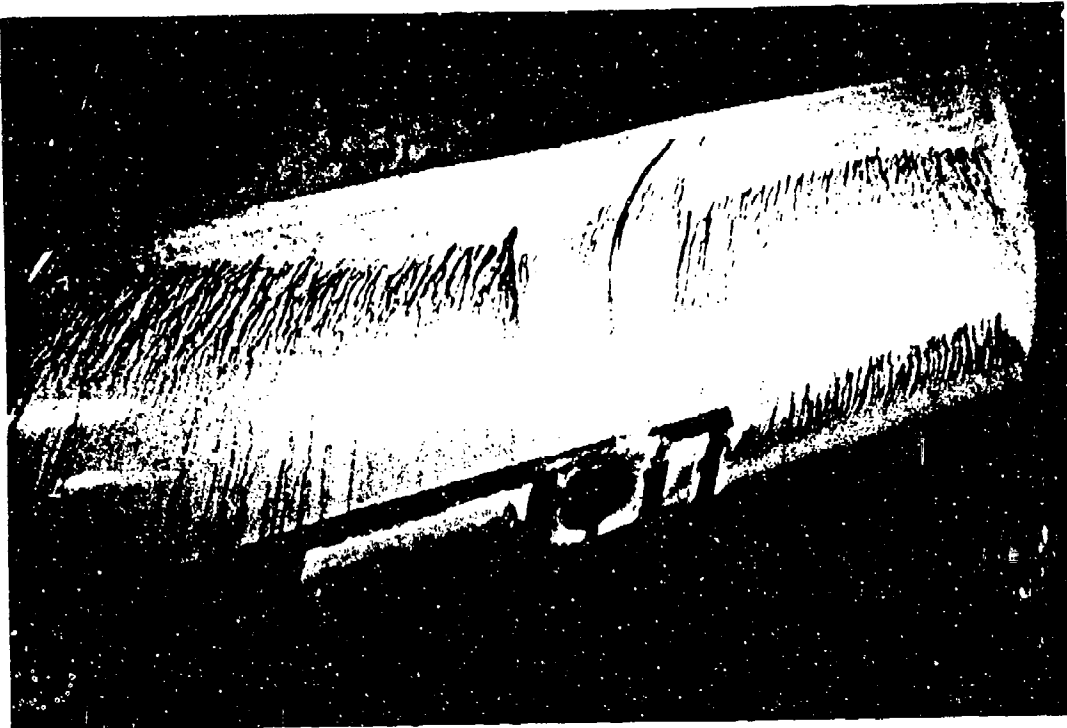
Figure 21(c). Fluorescent Dye/Oil Smear Contours Associated with One Leading Edge Insert Opening



$$\alpha = 36^\circ, C_L = 1.14$$

This flow pattern shows two characteristics associated with the modification generated vortices as the angle of attack is increased. Compared with the pattern generated at $\alpha = 33^\circ$, (1) the angle between the vortex axes has increased, (2) the distance between the air wing surface and the vortex axis increases causing a wider but shorter area under the axes to experience a decreased effective angle of attack.

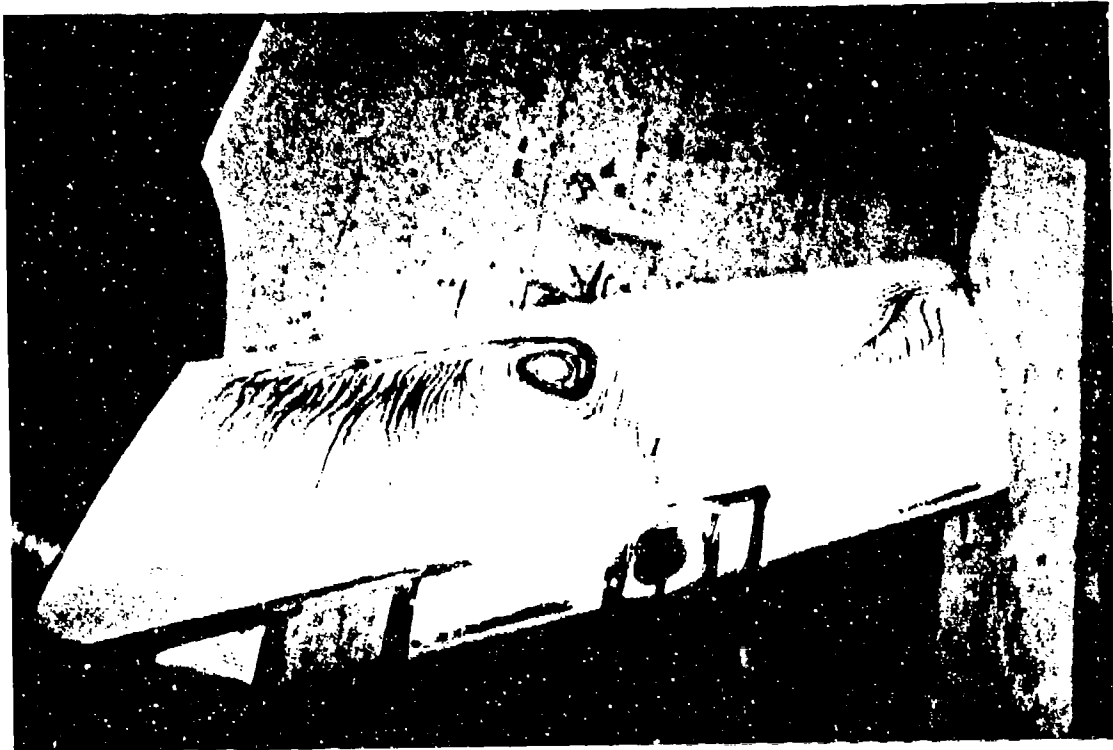
Figure 21(d). Fluorescent Dye/Oil Smear Contours Associated with One Leading Edge Insert Opening



$$\alpha = 8^\circ, C_L = .66$$

This flow picture shows the smear profile in the process of being developed. The chordwise streaks indicate that this dye-oil material is being moved rearward by the flow field. Where the streaking stops, toward the trailing edge, separation is indicated. The initial formation of vortices is seen behind the outboard modification opening. A very narrow band of separated flow extends rearward between the vortices formed by the outward modification opening. No vortex formation is evident at the inboard modification.

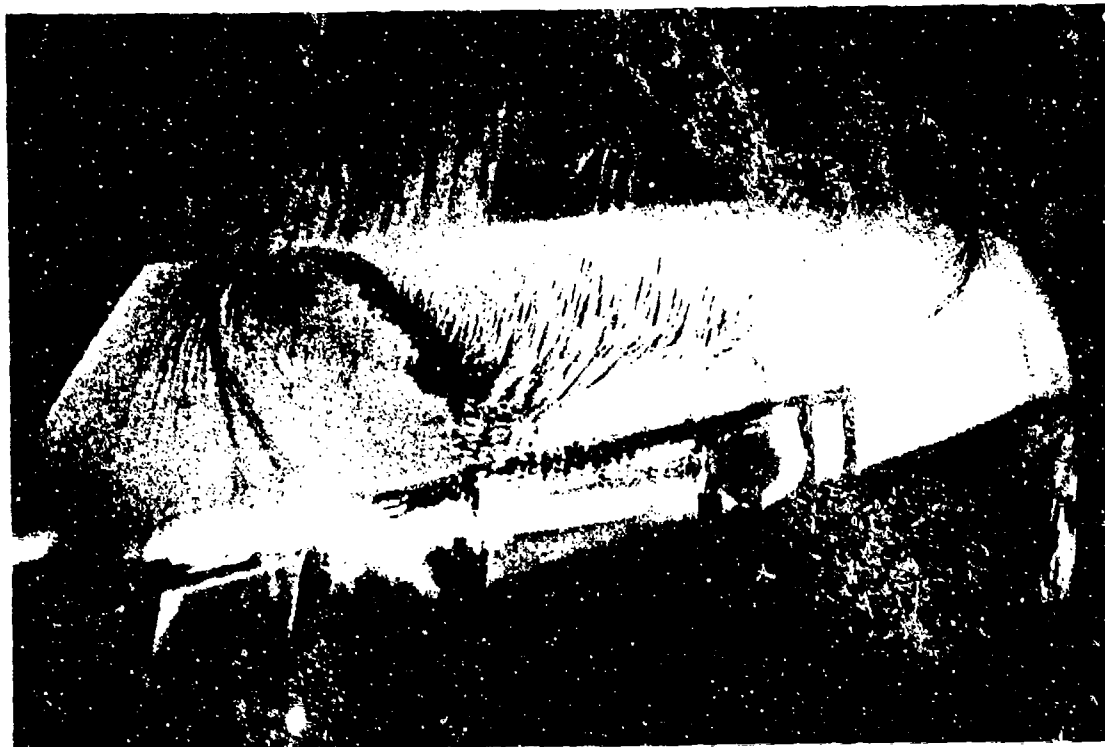
Figure 22(a). Fluorescent Dye/Oil Smear Contours Associated with Two Leading Edge Insert Openings



$$\alpha = 22^\circ, C_L = 1.23$$

A significant change in the dye-oil pattern has occurred as the angle of attack is increased from 8 to 22 degrees. The vortices developed by the outboard modification appear to be well developed. They diverge from the opening chordwise centerline with an accompanying separated flow region between them. Spanwise flow has developed at the inboard trailing edge region. This flow feeds into the separated flow region existing between the modification generated vortex pair. No vortex development is evident at the inboard modification.

Figure 22(b). Fluorescent Dye/Oil Smear Contours Associated with Two Leading Edge Insert Openings



$$\alpha = 25^{\circ}, \quad C_L = 1.25$$

Increasing the angle of attack from 22 to 25 degrees has caused a significant increase in the separated flow area covering the center section of the wing. The flow streaks show that reverse flow exists in this center section area from the trailing edge to the mylar tape strip (9.22 cm from the leading edge). This streak pattern also shows evidence of a strong vortex existing from the outboard side of the outboard modification opening. The influence of this vortex is keeping the flow attached on a significant portion of the outer wing section. No evidence of vortex development can be observed at the inboard modification or from the inboard side of the outboard location.

Figure 22(c). Fluorescent Dye/Oil Smear Contours Associated with Two Leading Edge Insert Openings

APPENDIX A

**Master List of Tests Conducted to Study the Effects of
Leading-Edge Modifications on the Straight Planform Wing Model**

<u>Run No.</u>	<u>Modification Designation</u>	<u>Remarks</u>
227	Baseline wing, no modification	
228	Insert #12 at mid-semispan location Insert #1 at wing root location	Teardrop insert modification Opening spanwise dimension = 4.92 cm Opening chordwise dimension = 7.30 cm
229	Insert #13 at mid-semispan location Insert #1 at wing root location	Teardrop insert modification Opening spanwise dimension = 5.40 cm Opening chordwise dimension = 6.67 cm
230	Insert #14 at mid-semispan location Insert #1 at wing root location	Teardrop insert modification Opening spanwise dimension = 4.45 cm Opening chordwise dimension = 4.76 cm
231	Insert #17(a) at mid-semispan location <u>Note:</u> This insert configuration was used as a model for the gap opening test insert (#17(b)). Upon starting the chordwise opening test series, it was determined that the contouring of the opening's lateral side areas could not be fabricated to model this feature of insert #17(a). Thus the data of insert #17(a) were not included in the chordwise opening test results.	Wing stub thickness = 60% Wing stub gap = 0.84 cm Opening spanwise dimension = 8.33 cm Opening chordwise dimension = 2.70 cm

232(a)	Insert #17(b) at mid-semispan location	Wing stub thickness = 60% Wing stub gap = 0.84 cm Opening spanwise dimension = 8.33 cm Opening chordwise dimension = 0.16 cm
232(b)	Insert #17(b) at mid-semispan location	Wing stub thickness = 60% Wing stub gap = 0.84 cm Opening spanwise dimension = 8.33 cm Opening chordwise dimension = 0.32 cm
233(a)	Insert #17(b) at mid-semispan location	Wing stub thickness = 60% Wing stub gap = 0.84 cm Opening spanwise dimension = 8.33 cm Opening chordwise dimension = 0.48 cm
233(b)	Insert #17(b) at mid-semispan location	Wing stub thickness = 60% Wing stub gap = 0.84 cm Opening spanwise dimension = 0.833 cm Opening chordwise dimension = 0.64 cm
233(c)	Insert #17(b) at mid-semispan location	Wing stub thickness = 60% Wing stub gap = 0.84 cm Opening spanwise dimension = 8.33 cm Opening chordwise dimension = 0.79 cm

APPENDIX B

Master List of Tests Conducted on the 30° Swept Wing for which a Complete Data Analysis was Obtained

<u>Run No.</u>	<u>Modification Designation</u>
234	Baseline wing, no modifications
235	Baseline wing with wing root modification
236	Baseline wing with wing root modification
237	Baseline wing with wing root modification
238	Insert #26 at 6B/7B; no wing root modification
239	Insert #25 at 6B/7A; no wing root modification
240	Insert #25 at 6B/7A; no wing root modification
241	Insert #26 at 5B/6A; no wing root modification
242	Insert #26 at 6A/6B; no wing root modification
243	Insert #30 at 5B/6A; no wing root modification
244	Insert #30 at 5B/6A; insert #28 at 1A
245	Insert #26 at 6A/6B; insert #30 at 1B/2A
246	Insert #26 at 6A/6B; insert #20 at 1A/1B
247	Insert #26 at 6A/6B; insert #30 at 2A/2B
248	Insert #26 at 6A/6B; insert #30 at 2B/3A
249	Insert #26 at 6A/6B; insert #30 at 3A/3B
250	Insert #26 at 6A/6B; insert #30 at 3B/4A
251	Insert #26 at 6A/6B; insert #30 at 4A/4B
252	Insert #26 at 6A/6B; insert #30 at 3A/3B
253	Insert #25 at 6A/6B; insert #30 at 3A/3B
254	Insert #26 at 6B/7A; insert #25 at 3B/4A
255	Insert #26 at 6B/7A; insert #30 at 3B/4A
256	Insert #26 at 6B/7A; insert #30 at 3B/4A
257	Insert #26 at 6B/7A; insert #30 at 3B/4A
258	Insert #26 at 6B/7A; insert #30 at 3B/4A
259	Insert #26 at 6B/7A; insert #30 at 3A/3B

- 260 Insert #26 at 6B/7A; insert #30 at 4A/4B
- 261 Baseline wing, no modifications
(Leading edge sections 1A to 7A held in place with mylar tape)
- 262 to 266 Insert #26 at 6A/6B; insert #30 modified at 3A/3B
- 267 to 270 Insert #26 modified at 6A/6B; insert #30 modified at 3A/3B
- 271 and 272 Insert #31 modified at 6A/6B; insert #30 modified at 3A/3B
- 273 Insert #26 modified at 6A/6B; insert #30 modified at 3A/3B
- 274 and 275 Insert #31 modified at 6A/6B; insert #30 modified at 3A/3B
- 276 Insert #31 modified at 6A/6B; insert #30 modified at 3A/3B
(Low Reynolds Number test of modified wing)
- 277 Baseline wing, no modifications
(Low Reynolds Number test of baseline wing)

DISTRIBUTION LIST

NAVAIRSYSCOM	AIR-320D	3 copies
	AIR-5301	4 copies
DTNSRDC	1606	10 copies
DTIC		12 copies